



# รายงานวิจัยฉบับสมบูรณ์

## โครงการ การศึกษาเปรียบเทียบอุปกรณ์ FACTS อย่างละเอียด ในการเพิ่มเสถียรภาพแรงดันในสภาวะคงตัว

โดย ดร.อาทิตย์ โสตรโยม

# รายงานวิจัยฉบับสมบูรณ์

โครงการ การศึกษาเปรียบเทียบอุปกรณ์ FACTS อย่างละเอียด ในการเพิ่มเสถียรภาพแรงดันในสภาวะคงตัว

คณะผู้วิจัย ดร.อาทิตย์ โสตรโยม สังกัด มหาวิทยาลัยสยาม

สนับสนุนโดยสำนักงานคณะกรรมการอุดมศึกษา และสำนักงานกองทุนสนับสนุนการวิจัย (ความเห็นในรายงานนี้เป็นของผู้วิจัย สกอ. และ สกว. ไม่จำเป็นต้องเห็นด้วยเสมอไป)

## Acknowledgements

Author would like to express his sincere appreciation, gratitude and indebtedness to Thailand Research Fund (TRF) and Office of Higher Education Commission for the financial support. Without the support from them, he think that he could not complete his research.

The author deeply acknowledges mentors, namely Dr. Nadarajah Mithulananthan (Senior Lecturer, School of Information Technology and Electrical Engineering, University of Queensland, Australia) and Professor Dr. Kwang Y. Lee (Head of Electrical and Computer Engineering Department, Baylor University, USA) for their help, suggestion and valuable guidance to make this work more valuable to research.

Author wishes to express his deep appreciation to Siam University, Thailand, for the financial support to attend international and national conferences.

Last but not least, the author would like to give most of the gratitude to his parents for making their son succeeded during the first part of his life. Good things are given to my past away father for his sacrifice.

Arthit Sode-Yome

#### Abstract

Voltage instability has been a major concern in power systems, especially in planning and operation, as there have been several major power interruptions associated with this phenomenon, in the recent past. Voltage instability due to the lack of the ability to foresee the impact of contingencies is one of the main reasons for the worst North American power interruptions on August 14th, 2003. Hence, electric power utilities around the world have been devoting a great deal of efforts in voltage stability assessment and margin enhancement.

Major contributory factors to voltage instability are power system configuration, generation pattern and load pattern. Power system network can be modified to alleviate voltage instability by adding reactive power sources i.e. shunt capacitors and/or Flexible AC Transmission System (FACTS) devices at the appropriate locations. There are various types of FACTS devices, namely Static Var Compensator (SVC), Static Synchronous Compensator (STATCOM), Thyristor-Controlled Series Capacitor (TCSC), Static Synchronous Series Compensator (SSSC) and Unified Power Flow Controller (UPFC). Each of these FACTS devices, however, has its own characteristics and limitations. Adequate representations of FACTS devices have a great impact on voltage stability margin. Moreover, appropriate type, placement and correct size of the devices are important and become necessary for power system, especially in a de-regulated environment, to achieve maximum loading margin and other benefits.

Based on the above observation, attention is drawn in this research to study the influence of FACTS devices on static voltage stability margin. The work investigates and compares various types of FACTS devices in terms of static voltage stability margin. Appropriate model is used to represent AC and DC characteristics and limitations of FACTS devices. New placement and sizing techniques of these devices are also proposed to provide a higher voltage stability margin.

The IEEE test system is used for testing and validating all the proposed methodologies. Moreover, a new idea on voltage setting of existing FACTS devices is also proposed to provide the highest margin in the test systems.

## **Table of Contents**

CHAP	PAGE	
	Title Page	i
	Acknowledgements	ii
	Abstract	iii
	Table of Contents	iv
	List of Terms	vi
	List of Figures	ix
	List of Tables	X
1	Introduction	1
	1.1 Introduction	1
	1.2 Research Motivation	2
	1.3 Literature Review	2 2 2
	1.3.1 Static Voltage Stability	2
	1.3.2 Network Improvement	3 5
	1.4 Research Objectives	5
	1.5 Outline of Report	5
2	Modeling, Tools and Test Systems	6
	2.1 Introduction	6
	2.2 Static Voltage Stability Study	6
	2.2.1 Overview	6
	2.2.2 Analysis Techniques	8
	2.2.3 Voltage Stability Margin Enhancement	14
	2.3 FACTS Devices	14
	2.3.1 SVC	15
	2.3.2 STATCOM	17
	2.3.3 TCSC	20
	2.3.4 SSSC	22
	2.3.5 UPFC	23
	2.4 Analysis Tools	26
	2.5 Test Systems	27
	2.5.1 IEEE 14-Bus Test System	27
	2.5.2 Modified IEEE 14-Bus Test System	28
	2.6 Summary	28
3	Influence of FACTS Controllers	29
	3.1 Introduction	29
	3.2 Shunt FACTS Controllers	29
	3.2.1 Placement	30
	3.2.2 Suitable Size	30
	3.2.3 PV Curves and Voltage Profiles	31

## **Table of Contents (Cont'd)**

CHAPTER TITLE		PAGE	
		3.2.4 Power Losses	33
		3.2.5 Contingency	35
	3.3	Series FACTS Controllers and UPFC	35
		3.3.1 Placement	36
		3.3.2 Suitable Size	38
		3.3.3 PV Curves and Voltage Profiles	43
		3.3.4 Power Losses	45
		3.3.5 Contingency	47
	3.4	1	47
		3.4.1 PV Curves and Voltage Profiles	47
		3.4.2 Power Losses	49
		3.4.3 Contingency	51
	3.5	Summary	51
4	Con	clusion	52
	4.1	Concluding Observations	52
	4.2	Main Contributions	53
	4.3	Future Directions	53
	Bibl	liography	54
	Appe	endix A IEEE 14-Bus Test System	59
		endix B FACTS Controller Data	63

#### **List of Terms**

## **Acronyms:**

CPF : Continuation Power Flow

DAE : Differential Algebraic Equation
EPRI : Electric Power Research Institute

FACTS : Flexible AC Transmission System

HVDC : High Voltage Direct Current

IEEE : Institute of Electrical and Electronics Engineers

IPP : Independent Power Producer

J : Jacobian

LD : Load Direction

LF : Loading Factor

LM : Loading Margin

PWM : Pulse Width Modulation

SSSC : Static Synchronous Series Compensator

STATCOM : Static Synchronous Compensator

SVC : Static Var Compensator

TCR : Thyristor-Controlled Reactor

TCSC : Thyristor-Controlled Series Capacitor

UPFC : Unified Power Flow Controller

UWPFLOW: University of Waterloo Power FLOW

## **Symbols:**

z : System state and algebraic variables

 $\lambda$  : Loading Factor

V : Voltage magnitude

 $\delta$  : Phase angle

w : Left eigenvector

W : Left eigenvector matrix U : Right eigenvector matrix  $\Sigma$  : Matrix of singular values

 $B_e$  : Total susceptance

 $B_{max}$  : Maximum susceptance  $B_{min}$  : Minimum susceptance  $\alpha$  : Firing angle of thyristor

 $X_L$  : Inductance  $X_C$  : Capacitance

I: Injected current  $V_i$ : Terminal voltage

 $P_{ref}$  : Controlled active power  $Q_{ref}$  : Controlled reactive power

 $\beta$  : Phase angle of internal voltage

 $V_{dc}$  : DC voltage

*m* : Modulation index

 $\alpha_v$ : Angle of internal synchronous source

 $R_c$ : Internal DC losses

 $\theta$  : Angle of current se : Series component sh : Shunt components

*l* : Line used for current and power flow control

 $\partial Q_{loss}/\partial \lambda$  : Reactive power loss sensitivity

 $K_{Gi}$ : Generation Direction of generator i

 $P_{Gi}$ : Power generation of generator i  $Q_{Gi}$ : Reactive generation of generator i

 $P_{Gi,o}$ : Generation of generator i at base load

 $P_{Di,o}$  Real power demand at bus i at base load

 $Q_{Di,o}$  : Reactive power demand at bus i at base load

 $\Delta P_{Gi}$ : Increase of power generation at generator i

 $\Delta P_D$  : Total load increase  $\Delta P_{Loss}$  : Total loss increase

*NG* : Number of generators

## **List of Terms (Cont'd)**

*n* : Number of buses in the system

 $|P_{Gi}|_{min}$ : Lower power limits of generator i

 $/P_{Gi/max}$ : Upper power limits of generator i

 $|U_i|_{min}$ : Lower limits of voltage magnitude at bus i

 $/U_{i/max}$ : Upper limits of voltage magnitude at bus i

 $P_{ij}$ : Real power in line ij

 $Q_{ij}$  : Reactive power in line ij

 $S_{ij}$ : Apparent power in line ij,

 $S_{ij,max}$ : MVA (Thermal) limit of line ij.

LM : Loading margin

## **Table of Figures**

FIGURE	TITLE	PAGE
2.1	Continuation method geometry in state space and parameter space.	11
2.2	Basic structure of SVC.	16
2.3	Basic structure of STATCOM.	18
2.4	Basic structure of TCSC.	20
2.5	Basic structure of SSSC.	22
2.6	UPFC configuration.	24
2.7	Single line diagram of the IEEE 14 bus system.	27
2.8	Single line diagram of the modified IEEE 14 bus system	28
3.1	Loading margin vs controller capacities for shunt controllers.	31
3.2	PV curves of Base case, with various shunt FACTS controllers.	32
3.3	Voltage Profiles of each bus at LM for Base case and different	
	controllers.	33
3.4	Real power losses in the system for different shunt controllers.	34
3.5	Reactive power losses in the system for different shunt controllers.	34
3.6	Capacity of TCSC at various LFs.	39
3.7	Active power capacity of SSSC at various LFs.	39
3.8	Reactive power capacity of SSSC at various LFs.	40
3.9	P <sub>se</sub> of UPFC at various LFs.	41
3.10	P <sub>sh</sub> of UPFC at various LFs.	41
3.11	Q <sub>se</sub> of UPFC at various LFs.	42
3.12	Q <sub>sh</sub> of UPFC at various LFs.	42
3.13	PV curves of base case. with TCSC and SSSC at line 1-5.	43
3.14	PV curves of base case, with UPFC at line 9-14.	44
3.15	Voltage profile of base case, with TCSC, SSSC and UPFC.	45
3.16	Real power losses of the system with STATCOM, SSSC and UPFC.	46
3.17	Reactive power losses of the system with TCSC, SSSC and UPFC.	46
3.18	PV curves of base case, with FACTS devices.	48
3.19	Voltage profile of base case, with FACTS devices.	49
3.20	Real power losses of the system with FACTS devices.	50
3.21	Reactive power losses of the system with FACTS devices.	50

## **Table of Tables**

TABLE TITLE		PAGE	
2.1	Cost comparison of shunt controllers	15	
3.1	Tangent vector of the first four weakest buses	30	
3.2 3.3	LM and % Increase of LM for base case, with SVC and STATCOM Loading Margin for various line outages for base case and different	32	
	controllers	35	
3.4	Tie Line Index near LM of IEEE 14 bus test systems in normal		
	condition	36	
3.5	Tie Line Index near LM of IEEE 14 bus test system with N-1 (Line		
	2-3)	37	
3.6	Loading Margin of Base case and system with TCSC connected	38	
3.7	Loading Margin and % Increase of LM of base case and system with		
	TCSC, SSSC and UPFC.	44	
3.8	Loading Margin for various line outages for base case and different		
	controllers	47	
3.9	LM and % Increase of LM of base case, with FACTS devices	48	
3.10	Loading Margin for various line outages for base case and various		
	FACTS controllers	51	

## Chapter 1

#### Introduction

#### 1.1 Introduction

Modern electric power utilities are facing many challenges due to ever-increasing complexity in their operation and structure. In the recent past, one of the problems that receive wide attention among utilities has been the voltage instability [1]-[3]. With the lack of new generation, transmission facilities and over exploitation of the existing facilities geared by increase in load demand make these types of problems are more likely to happen in the modern power systems.

In recent decades, several major voltage instability have been observed and reported in many countries such as France, Belgium, Sweden, Germany, Japan, the United States, etc [4],[5]. Voltage instability is the cause of voltage collapse, which results in wide spread power interruptions. Voltage instability due to the lack of ability to foresee the impact of contingencies is the main reason for the worst North American power interruption on August 14th, 2003. In this incident, reports indicate that approximately 50 million people were interrupted from the continuous supply of power for more than 15 hours [5]. Moreover, with an open-access market, poorly scheduled generation from the competitive bidding is one of many reasons for voltage instability problem in the deregulated electricity environment.

Voltage instability is the inability of the power system to transfer reactive power to the load due to exhaustion of the reactive power sources or enormous reactive power losses in the transmission system. It is mainly associated with reactive power imbalance. In voltage stability study, slowly developing changes in the power system occur that eventually lead to a shortage of reactive power and declining voltage. At the collapse point or maximum voltage stability margin, reactive power is out of use such that the voltage is sharply decreased and finally collapsed. The maximum load that can be supplied prior to the point at which the system reactive power is out of use is called static voltage stability margin or loading margin (LM) of the system. Voltage instability and collapse in practical power systems can be avoided by increasing the static voltage stability margin. This can be done by adjusting factors that principally contribute to it.

Major contributory factors to voltage instability are power system configuration, generation pattern, and load pattern [1]-[4],[6]-[11]. Power system network or topology can be modified to alleviate voltage instability by adding reactive power sources i.e. shunt capacitors or Flexible AC Transmission System (FACTS) devices at the appropriate location [11]-[12]. Impact of generation pattern and load pattern on static voltage stability can be found in references [22]-[30].

#### 1.2 Research Motivation

Power system network can be modified to enhance voltage stability margin by introducing FACTS devices in the transmission system. There are various types of FACTS devices available for this purpose, namely, Static Var Compensator (SVC), Static Synchronous Compensator (STATCOM), Thyristor-Controlled Series Capacitor (TCSC), Static Synchronous Series Compensator (SSSC) and Unified Power Flow Controller (UPFC) [14]. Each of these FACTS devices, however, has its own characteristics and limitations [11]. Appropriate models of these FACTS devices including AC and DC representation may be required to represent all the behaviors and limitations of the devices, especially when they are operated at the limits [11],[15],[16]. Moreover, optimal placement and sizing of these FACTS devices are important issues. Placing FACTS devices with the appropriate sizes may enhance voltage stability of the system in an optimal way [17]-[21]. According to these, it would be useful to study and compare these five well-known FACTS devices, namely SVC, STATCOM, TCSC, SSSC and UPFC, with appropriate representation in the same test system. Moreover, some techniques to provide optimal locations and sizes of these FACT devices could be proposed to provide their optimal uses.

#### 1.3 Literature Review

## 1.3.1 Static Voltage Stability

Concerns on voltage instability have come into attention to many utilities and researchers for several decades. Started in 1990, the energy function method has been proposed in [31], which defines a security measure to indicate vulnerability to voltage collapse. In 1993, another approach is presented in [7] based on singular value decomposition of load flow Jacobian matrix and matrices derived from the Jacobian matrix. Later, this method has been practically applied to large-scale power system in [1], which presents the development of systematic approach to voltage stability assessment of large-scale power systems using both static and dynamic techniques. In this study, modal analysis at the "nose point" of PV curve is used to identify the SVC location. In [8], the modal analysis method is further applied to AC-DC system with HVDC facility.

Continuation power flow method is proposed for the computation of voltage collapse points in large AC/DC power systems in [32] and [33]. Continuation power flow method yields voltage sensitivity information and time performance that justify its use as a production tool. It appears particularly promising when HVDC lines with controller limits are considered. Tangent vector method is proposed in [34] to identify the weakest bus, based on the largest tangent vector component as a function of load increase. The explicit advantage of this method is to provide less computational effort, since the tangent vector components are calculated as a predictor step in continuation power flow process. Later, in order to compare all available methods, reference [35] studies and discusses some voltage collapse indices, namely singular value decomposition, eigenvalue decomposition, reduced Jacobian determinant, test function and tangent vector. The results obtained confirm that the tangent vector is a more promising voltage security index [34],[35].

The establishment of novel method for the study of voltage stability is performed in the following literatures. Reference [36] proposes a new method of finding voltage stability limit in P-Q plane. Equations are required to generate the voltage stability boundary using the exact transmission line model. Likewise, reference [37] proposes a novel method of determining various stability margins of critical bus or area in a large power system using the boundary of voltage stability of critical bus in P-Q plane. In [38], the derivation of the simple analytical expression for S-V (MVA-voltage) and expression for maximum MVA, MW and MVAR limitation through the exact representation of line with ABCD parameter is succeeded. Another methodology based on local measurement on bus voltage and load current to estimate the proximity to voltage collapse is presented in [39]. In this methodology, the voltage collapse assumes to happen when apparent impedance equals thevenin impedance.

Based on the literatures reviewed above, it becomes evident that the conventional methods used to investigate the static voltage stability could be classified as test function, modal analysis, sensitivity, and tangent vector methods. These methods can effectively analyze the large-scale power system regarding to voltage stability and they could be considered as indicators to predict the distance to voltage collapse or loading margin in the study of voltage stability assessment. Beside the conventional methods, other methodology i.e. P-Q plane and Z<sub>thevenin</sub> techniques could be adapted for the voltage stability study. The novel method, however, has limitations when a practical size power system is considered. Compared with other conventional methods, tangent vector method based on Continuation Power Flow (CPF) process is considered as the most promising approach, since it is based on load flow calculation at various load increase or loading factor (LF). Moreover, CPF method can provide completed PV curves as well as voltages at various loading factors.

## 1.3.2 Network Improvement

Stability Enhancement with FACTS Devices

FACTS devices have been used to increase voltage stability margin for the past several years. One of the early literatures proposed is reference [40] that describes the applications of FACTS to improve voltage and transient stabilities. These applications are shown to offer the potential for enhancing the system's stability margin. In [41], contributions are made on selection of SVC parameters such as controller gains, droop slopes, reference voltages and compensator ratings needed for voltage stability improvement. Reference [42] proposes transient stability models of STATCOM and SSSC, which are also suitable for voltage stability enhancement. Examination on the use of TCSC for stability improvement of power systems is also presented in [43]. Importantly, reference [44] describes the UPFC function in resolving voltage and thermal loading concern in planning studies. With the help of UPFC, the new 138 kV line approaches the effectiveness of an uncompensated 345 kV line.

Appropriate models of FACTS including control and operating limits are necessary for the voltage stability study. In [15], detailed steady-state models with control of SVC and TCSC to study their effects on voltage collapse phenomena in power systems are presented. Further, reference [45] investigates modeling technique appropriate for representing the UPFC. For well-known FACTS devices, reference [16] presents transient

stability and power flow models of SVC, STATCOM, TCSC, SSSC and UPFC suitable for voltage and angle stability studies.

Very scant research attention has been focused on appropriate models of FACTS devices in voltage stability study. More research attention should be placed on voltage stability with appropriate model of all FACTS controllers so that the behaviors and limits of the devices can be captured and their impact on voltage stability can be studied. This could provide more accurate reflections of FACTS devices in the stressed system conditions, especially when the devices are operated at their limits. The study should also compare all available FACTS devices in terms of voltage stability margin in the same system to see and rank them based on their performance and cost. This provides a useful information for utilities to select the most appropriate FACTS device in context of voltage stability. Merits and demerits of all FACTS devices could also be revealed in regard to voltage stability.

## Locations of FACTS Devices

Very few literatures consider the placement of FACTS devices, especially series FACTS devices and UPFC. Reference [46] showed that optimum location of FACTS in the lossless transmission line could be sited at the mid-point of the line. The ability to transfer power is double that of uncompensated line. Likewise, for the practical transmission system, reference [18] proposes that FACTS devices should be placed slightly off-center (L=0.45) to get the highest possible benefit, which is the increase of both power transfer capability and stability of the system. Reference [47] presents reactive power losses sensitivity method to find the placement of SVC and TCSC. The study, however, does not consider placement for STATCOM, SSSC and UPFC. In addition, DC representation is not considered in the study. In [48], a novel method called Extended Voltage Phasors Approach (EVPA) for placement of FACTS devices in power systems is presented. The technique, however, may be problematic when a large-scale power system is considered.

After the layout of FACTS application in voltage stability study, it is clear that the obvious shortcomings that need more research attention are the placement of the series FACTS devices and UPFC. Factors that limit the locations the devices in practical power systems, such as available space, voltage level etc., should be considered. Placement technique should be more clarified, especially, for large-scale power system planning.

## Sizes of FACTS Devices

Another important aspect of FACTS application for static voltage stability margin is the appropriate size of FACTS. Quite a few studies focus on this issue, reference [19] proposes a method for placement and sizing of SVC. The placement of SVC is based on the voltage sensitivity, which results in effect in voltages at as many buses as possible. The size of SVC is found based on an optimization technique. In [17], a new methodology to find SVC location and suitable size was achieved based on L index of load buses and amount of reactive power required, respectively. The approach also leads to the improved voltage and minimum loss condition.

As seen from summarized literatures, only a few research contribution has been paid to this particular area. Attention should be paid to find appropriate sizes of STATCOM, TCSC, SSSC and UPFC.

## 1.4 Research Objectives

The objectives of this research are to study the influence of FACTS controllers in static voltage-stability margin. The specific objectives of this research is to study static voltage stability of power system, including well-known FACTS devices with appropriate model, namely SVC, STATCOM, TCSC, SSSC and UPFC. The study also includes placement and sizing issues of FACTS controllers.

## 1.5 Outline of Report

The report is structured as follows:

- Chapter 2 presents concepts and mathematical representation of power system for static voltage stability study with FACTS devices. Analysis tools and test systems used in this study are also presented.
- Chapter 3 presents the influence of FACTS devices in static voltage stability.
- Finally, Chapter 4 provides a summary, contribution and future work of the research.

## Chapter 2

## **Modeling, Tools and Test Systems**

#### 2.1 Introduction

Voltage stability can be broadly classified based on time frame of simulation into two categories: static voltage stability and dynamic voltage stability. In dynamic consideration, the study includes dynamic effects of equipment such as transformer tap changers, induction motor, load, etc., whereas static study considers load variation as a slow process over long period of time [3],[4]. Most of the problem found in power system realizes voltage collapse as a static phenomenon [3],[4]. Static study involves only the solution of algebraic equations and therefore is computationally less extensive than dynamic analysis. It is appropriate for a bulk power system study, which involves enormous number of buses and generators [3]. Accordingly, the research conducted in this study is concentrated only in static voltage stability.

Mathematical models for static voltage stability study consist of load flow equation, singularity condition of load flow Jacobian and the equation for non-zero left eigenvectors. There are many analysis techniques and tools used for static voltage stability study. Moreover, if FACTS device with appropriate AC and DC representation is introduced in the power system, more equations are added in voltage stability study. This chapter presents static voltage stability study including overview, mathematics representation and analysis techniques. Mathematical representation of all FACTS devices in static voltage stability study is presented. Moreover, analysis tools and the test systems used throughout this study are also presented.

This chapter is organized as follows. Section 2.2 introduces static voltage stability. In Section 2.3, stability models and mathematical representation of all FACTS devices are summarized. These models are introduced in static voltage stability study. In Section 2.4, analysis tools that are used throughout the study are presented. Section 2.5 mentions, in brief, about the test systems including the IEEE 14-bus test systems that has been used to test all the proposed methodology. Finally, a summary of the chapter is given in Section 2.6.

### 2.2 Static Voltage Stability Study

#### 2.2.1 Overview

Static voltage instability is mainly associated with reactive power imbalance. Reactive power support that the bus receives from the systems can limit loadability of that bus. If the reactive power support reaches the limit, the system will approach the maximum

loading point or voltage collapse point due to high real and reactive power losses [1]-[4],[11]. Accordingly, the reactive power supports should be local and adequate in order to avoid problem associated with its transmission, especially in a stressful condition.

In static voltage stability, slowly developing changes in the power system occur that eventually lead to a shortage of reactive power and declining voltage. This phenomenon can be seen from the plot of the voltage at receiving end versus the power transferred. The plots are popularly referred to as P-V curve or "Nose" curve. As the power transfer increases, the voltage at the receiving end decreases. Eventually, the critical (nose) point, the point at which the system reactive power is out of use, is reached where any further increase in active power transfer will lead to very rapid decrease in voltage magnitude. Before reaching the critical point, the large voltage drop due to heavy reactive power losses can be observed. The maximum load that can be increased prior to the point at which the system reactive power is out of use is called static voltage stability margin or loading margin of the system. The only way to save the system from voltage collapse is to reduce the reactive power losses in the transmission system or to add additional reactive power prior to reaching the point of voltage collapse. This has to be carried out in the planning stage with several system-wide studies.

Under normal operating conditions, power system exhibits slow dynamics, with transient oscillations of small amplitude compared with the overall change observed in a short time. Therefore, it is reasonable to assume a quasi-static condition. The typical quasi-steady-state description of a power system considered for static voltage stability analysis is given by the differential-algebraic equations (2.1) [3],[4].

$$\dot{x} = f(x, y, \lambda) 
0 = g(x, y, \lambda)$$
(2.1)

or

$$\begin{bmatrix} \dot{x} \\ 0 \end{bmatrix} = F(x, y, \lambda) = F(z, \lambda) \tag{2.2}$$

where z corresponds to a vector of the system state and algebraic variables and  $\lambda$  is the loading factor representing the percent increase in load.

In static voltage analysis, the equilibrium point is considered. At equilibrium point, the equation (2.2) is simplified to  $F(z_0, \lambda_0) = 0$ . Hence, an equilibrium point  $(z_*, \lambda_*)$  where determinant of Jacobian,  $dF(z_*, \lambda_*)/dz$ , becomes zero is known as a singular bifurcation point. This equilibrium point in power system has been directly associated with voltage collapse point [3].

The power flow model is used to identify the voltage stability indices as the power flow equation yields adequate results, as singularities in related power flow Jacobian can be associated with actual singular bifurcation of the corresponding dynamical system. The power flow model used to obtain different voltage stability indices is represented by the

typical load-flow vector nonlinear equation defined the active and reactive power mismatches at system buses, i.e.

$$F(u,\lambda) = \begin{bmatrix} \Delta P(u,\lambda) \\ \Delta Q(u,\lambda) \end{bmatrix} = 0 \tag{2.3}$$

where  $F(u,\lambda)$  is a subset of  $F(z,\lambda)$ , with under quasi-static condition u typically representing V and  $\delta$ , voltages and phase angles, respectively.

The system load change drives the system to collapse in the following way:

$$P_{D,i} = P_{o,i} \left( 1 + \lambda K_{P,i} \right)$$

$$Q_{D,i} = Q_{o,i} \left( 1 + \lambda K_{Q,i} \right)$$
(2.4)

where  $P_{o,i}$  and  $Q_{o,i}$  represent the initial active and reactive loads at bus i and constants  $K_{P,i}$  and  $K_{O,i}$  represent the active and reactive load increase direction of bus i, respectively.

In summary, for the voltage stability study, the power flow model is used, where the variations of constant active and reactive power loads are assumed to be the main parameters driving the system to collapse point.

### 2.2.2 Analysis Techniques

The purposes of analysis techniques are to identify system conditions causing voltage instability, to find loading margin of the system and to specify the parameters affecting the voltage stability of the system. In static voltage stability study, four analysis techniques are popularly used, namely, direct, modal analysis, continuation power flow and optimization technique methods.

#### Direct Method

Direct method uses power flow equations, singular conditions of power flow Jacobian and non-zero left eigenvectors to find the maximum loading point. These conditions are summarized in (2.5)

$$F(z,\lambda) = 0$$
 -> Power Flow Equation

$$\frac{dF(z,\lambda)^{T}}{dz} w = 0 \qquad -> \text{Singularity Condition}$$
 (2.5)

$$||w|| = 1$$
 -> Non-zero Left Eigenvector

where w is the left eigenvector. Direct method consists in solving equation (2.5) for z,  $\lambda$  and w, to directly obtain the collapse point  $(z_*, \lambda_*)$ . This method allows to directly determine the loading margin  $(\Delta \lambda = \lambda_* - \lambda_o)$  at any operating point defined by  $\lambda_o$ . An obvious disadvantage of this technique is the high computational cost, requiring good initial conditions. In addition, pertinent information between maximum loading margin  $\lambda$  and the base case  $\lambda_o$  is not available.

#### Modal Analysis Method

In standard power flow, the Jacobian (J) contains the first derivatives of the reactive power mismatch equation  $Q(z,\lambda)$  with respect to the voltage magnitude V. Hence, linearizing the steady state equation  $F(z,\lambda)=0$  at the equilibrium point  $(z_0,\lambda_0)$ ,

$$\Delta F(z,\lambda) = J\Delta z \tag{2.6}$$

$$\begin{bmatrix}
\Delta \hat{F}(\delta, V, \lambda) \\
\Delta Q(\delta, V, \lambda)
\end{bmatrix} = \begin{bmatrix}
\frac{\partial \hat{F}(\delta_{0}, \lambda_{0})}{\partial \delta} & \frac{\partial \hat{F}(\delta_{0}, \lambda_{0})}{\partial V} \\
\frac{\partial Q(\delta_{0}, \lambda_{0})}{\partial \delta} & \frac{\partial Q(\delta_{0}, \lambda_{0})}{\partial V}
\end{bmatrix} \begin{bmatrix}
\Delta \delta \\
\Delta V
\end{bmatrix}$$

$$= \begin{bmatrix}
J_{1} & J_{2} \\
J_{3} & J_{4}
\end{bmatrix} \begin{bmatrix}
\Delta \delta \\
\Delta V
\end{bmatrix}$$
(2.7)

where  $\hat{F}(\delta, \lambda)$  represents the active power mismatch  $P(\delta, \lambda)$  [3].

The load flow Jacobian can be decomposed in such a way that

$$J = W \sum U^T \tag{2.8}$$

where W and U are the left and right eigenvector matrixes, respectively, and  $\Sigma$  is the matrix of singular values. Since matrix J represents the partial derivatives of the active and reactive power equations as a function of the state variables, one has:

$$\begin{bmatrix} \Delta \delta \\ \Delta V \end{bmatrix} = U \sum^{-1} W^T \begin{bmatrix} \Delta P \\ \Delta Q \end{bmatrix}$$
 (2.9)

If U and W hold the singular vectors, then  $\Sigma$  holds the singular values. When the system Jacobian becomes singular, the state variables present large variations for small load disturbances. This can be used for voltage stability study. When the system becomes stressed, the next incremental changes of load cause the voltage to dramatically reduce. The reduction in voltage further causes the large change in phase angle difference, which finally results in system voltage collapse. At the collapse point, load flow study provides no solution. The singularity of system Jacobian can be used as an indicator to detect proximity of voltage instability. Moreover, right and left eigenvectors, which are the decomposition of Jacobian, can reveal information related to the weakest bus and weakest area of the system.

## Continuation Power Flow Method

Continuation Power Flow (CPF) presents another way of determining proximity to voltage collapse point in power system. The method is an iterative method that can trace P-V curve of the system up to the maximum loading ("nose") point without having numerical problems. CPF overcomes some difficulties of successive power flow solution method, so they allow the user to trace the complete voltage profile by automatically changing the value of Loading Factor (LF or  $\lambda$ ). It involves predictor and corrector steps to guarantee a well behaved numerical solution of the related equation. PV curves are currently in use at some utilities for determining proximity to collapse so that operator can take timely preventive measures to avoid voltage collapse.

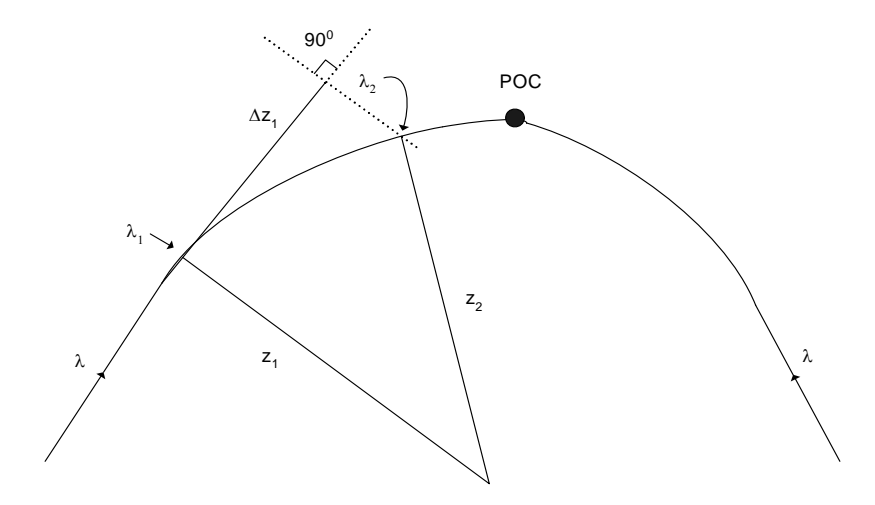


Figure 2.1: Continuation method geometry in state space and parameter space.

The CPF method uses the successive power flow solution to fully compute the voltage profiles up to collapse point to determine the loading margin. From Figure 2.1, assuming that the system is initially at the state  $(z_I, \lambda_I)$ , the predictor generates an initial guess  $(z_I+\Delta z_I, \lambda_I+\Delta\lambda_I)$  which is then used in the corrector step to compute a new equilibrium point  $(z_2, \lambda_2)$  on the system profile. To obtain the actual value of  $z_2$  and  $z_2$ , one can use the perpendicular hyperplane to the tangent vector to find the desired point in the branch. Tangent vector which is a byproduct of the CPF process can also be used as an index to identify the weakest bus of the system. Mathematically, the CPF procedure can be summarized in two steps, namely predictor and corrector steps [3],[32]-[33]. A third step known as parameterization is introduced to avoid some convergence problem [3].

#### Predictor

The direction vector  $\Delta z_I$  at the initial state  $(z_I, \lambda_I)$  on the system profile can be computed from the tangent vector to this trajectory at that point. At equilibrium point, the following relation can be applied:

$$\frac{dF}{d\lambda}(z_{1},\lambda_{1}) = \frac{dF}{dz}(z_{1},\lambda_{1})\frac{dz}{d\lambda}\Big|_{1} + \frac{\partial F}{\partial\lambda}\Big|_{1} = 0$$

$$\frac{dF}{dz}\Big|_{1}\frac{dz}{d\lambda}\Big|_{1} = -\frac{\partial F}{\partial\lambda}\Big|_{1}$$

$$\frac{dz}{d\lambda} = -\left[\frac{dF}{dz}\right]^{-1}\frac{\partial F}{\partial\lambda}\Big|_{1}$$
(2.10)

Thus, the direction vector and the parameter step come from the normalization of the tangent vector i.e.

$$\Delta \lambda_{1} = \frac{k}{\left\| \frac{dz}{d\lambda} \right\|_{1}} \tag{2.11}$$

$$\Delta z_1 = \Delta \lambda_1 \frac{dz}{d\lambda} \bigg|_{1} \tag{2.12}$$

where k is a scalar positive constant that controls the size of the predictor step. The normalization in equation (2.12) results in the reduction of the step size as the system approaches the collapse point, since the magnitude of the tangent vector increase as the system get closer to this point.

#### Corrector

Once the initial guess  $(z_I + \Delta z_I, \lambda_I + \Delta \lambda_I)$  is determined in the predictor step, the actual point  $(z_2, \lambda_2)$  on the system profile must be calculated by solving the following equations for z and  $\lambda$  from equations below.

$$F(z,\lambda) = 0$$

$$\rho(z,\lambda) = 0$$
(2.13)

where the first set of equations corresponds to the steady-state system equation and the second set of equations represents a condition that guarantees non-singularity at the bifurcation point.

### Parameterization

Parameterization technique may be used to avoid difficulty when the equilibrium point is close to the collapse point, since the system Jacobian becomes ill-conditioned. A simple technique is local parameterization, which is carried out simply by interchanging the parameter  $\lambda$  with the system variable z that has the largest normalized entry in the tangent vector, so that  $\lambda$  becomes part of the equation variables and z becomes the new parameter p, i.e.

$$p = \max \left\{ \left| \frac{\Delta z_i}{z_i} \right| , \left| \frac{\Delta \lambda}{\lambda} \right| \right\}$$
 (2.14)

As power system approaches the bifurcation, p changes from  $\lambda$  to the system bus voltage (z) that is varying the most, and after a few iterations of the method it returns back to  $\lambda$ .

## Optimization Technique Method

Static voltage stability study can be carried out by formulating the problem as an optimization problem [3]. Thus, distance to collapse can be maximized as follows:

Maximize

$$\lambda$$
 (2.15)

subject to

$$F(z,\lambda) = 0 (2.16)$$

This problem may be solved using Lagrangian

$$L(z,\lambda,w) = \lambda + w^{T} F(z,\lambda)$$
(2.17)

where w corresponds to the Lagrangian multipliers. Hence, necessary conditions to obtain a solution are

$$\frac{dL}{dw} = F(z,\lambda) = 0$$

$$\frac{dL}{dz} = \frac{dF(z,\lambda)^{T}}{dz} w = 0$$

$$\frac{dL}{d\lambda} = w^{T} \frac{\partial F(z,\lambda)}{\partial \lambda} + 1 = 0.$$
(2.18)

These equations are basically the same as equation (2.5), with the exception of the third one, which quarantees a nonzero w. Other power system limits such as voltage and thermal limits can also be introduced in the optimization formulation as an inequality constraint in (2.16).

Among the existing technique, CPF method is the most promising approach, since it is based on power flow calculation. It can provide complete PV curves as well as voltages at every bus at various loading factors, which can be used as an indicator to detect the proximity to voltage collapse. Thus, CPF method is used as an analysis tool for voltage stability assessment throughout the study.

## 2.2.3 Voltage Stability Margin Enhancement

Voltage instability of the system can be avoided by increasing voltage stability margin. Voltage stability margin can be enhanced by various ways i.e. by adding reactive power sources, increasing generation at the appropriate locations or reducing reactive power losses throughout the system. Introducing FACTS devices at the appropriate location is an effective way to increase voltage stability margin by adding reactive power where it is needed the most. It can be also viewed as a way to reduce reactive power losses, as the power flow is changed to less congested lines. In the following section, models and mathematics representation of FACTS devices that are used in this study are presented.

### 2.3 FACTS devices

The development of Flexible AC Transmission System (FACTS) controllers in power transmission system have led to many applications of these controllers not only to improve the stability of the existing power network but also to provide operating flexibility to the power system. FACTS controllers, developed by Electric Power Research Institute (EPRI) and Westinghouse Electric Corporation (Westinghouse), help utilities meet both the growing demand for electric power and the emerging challenges of open transmission access. The new devices, coupled with better computer and communications technology, offer the potential for enhanced system voltage stability both during the steady state operation and especially following system disturbance.

FACTS devices have been defined by the IEEE as "alternating current transmission system incorporating power electronic-based and other static controllers to enhance controllability and increase power transfer capability" [3],[14]. From the above definition, two main objectives of such devices can be restated as follows:

- To increase the power transfer capability of the transmission networks
- To provide direct control of power flow over designated transmission routes.

With these objectives, the FACTS controllers may provide significant benefits in terms of greater flexibility and extended stability margin of the power system.

To accomplish the objectives, FACTS devices increase the power system performance by delivering or absorbing real and/or reactive power. Although FACTS devices can offer high-speed control for enhancing power system, one disadvantage of power electronic

based controllers is their high cost per unit of rating compared to that of similar conventional equipment. Table 2.1 gives an idea about the cost of various FACTS controllers compared to that of shunt and series capacitors [14].

Table 2.1: Cost comparison of FACTS controllers

Shunt Controller	Cost (US \$)
Shunt Capacitor	8/kVar
Series Capacitor	20/kVar
SVC	40/ kVar controlled portions
TCSC	40/ kVar controlled portions
STATCOM	50/ kVar
UPFC Series Portions	50/ kVar Through power
UPFC Shunt Portions	50/ kVar controlled

Although FACTS devices are much more expensive than capacitor, they provide smooth and rapid response to secure power system during normal and abnormal operations. Shunt capacitor, on the other hand, provides coarse response and can not control voltage at the connected bus. Moreover, reactive power delivered by shunt capacitor is proportional to the square of voltage magnitude. Accordingly, these FACTS controllers are used for the stability improvement, especially for voltage stability.

In static voltage stability study, FACTS devices can be introduced into the formulation by adding equations of FACTS devices in the power flow equation. Conventionally, only AC equations are used. However, it may not provide a practical solution in the DC sides. Thus, appropriate model with AC and DC equations of each FACTS devices are important.

There are many types of FACTS controllers available in power systems. They can be connected to a transmission line at any appropriate location in series, in shunt or in a combination of series and shunt. The SVC and STATCOM are connected in shunt, whereas TCSC and SSSC are connected in series. UPFC, on the other hand, is connected in series and shunt combination. Each of FACTS devices has its own characteristic and limitations depending on its properties. They are represented by different models and mathematics equations. In the following subsections, static models and mathematical representation of all FACTS devices are presented.

#### 2.3.1 SVC

SVC is a shunt connected static Var generator/load whose output is adjusted to exchange capacitive or inductive current so as to maintain or control specific power system variables. SVC is similar to a synchronous compensator in that it is used to supply or absorb reactive power but without rotating part. It is also have the equivalent of automatic voltage regulator system to set and maintain a target voltage level. The basic structure of SVC is shown in Figures 2.2.

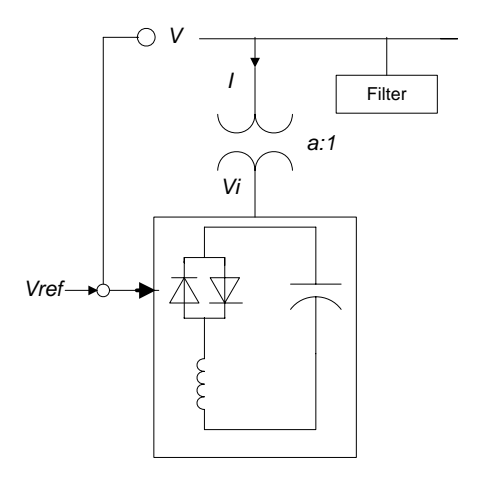


Figure 2.2: Basic structure of SVC.

SVC is composed of a controllable shunt reactor and shunt capacitor(s). Typically, the power system control variable controlled by SVC is the terminal bus voltage. Total susceptance ( $B_e$ ) of SVC can be controlled by controlling the firing angle ( $\alpha$ ) of thyristors. Consequently, it represents the controller with variable impedance that is changed with the firing angle of Thyristor-Controlled Reactor (TCR).

During the normal operation, the total susceptance can be controlled according to the terminal voltage. However, at limits, minimum or maximum susceptance, SVC behaves like a fixed capacitor or an inductor. At point  $B_{max}$ , all thyristor switched capacitor are switched on, with SVC providing rated capacitive current at specified voltage. At point  $B_{min}$ , the thyristor-controlled reactor is fully switched on, and all thyristor switched capacitors are off to give inductive current at a defined voltage.

SVC can increase voltage stability of the system by immediately providing reactive power support when the system has voltage problems such as due to a trip of an important generator or transmission line, etc.

Appropriate model including appropriate representation of SVC can be incorporated in static voltage stability study by adding SVC equations in the power flow equations. The validated p.u. Differential-Algebraic Equations (DAEs) corresponding to this model are [15]-[16]:

$$\begin{bmatrix} \dot{x}_c \\ \dot{\alpha} \end{bmatrix} = f(x_c, \alpha, V, V_{ref})$$
(2.19)

$$0 = \begin{bmatrix} B_{e} - \frac{2\alpha - \sin 2\alpha - \pi(2 - X_{L}/X_{C})}{\pi X_{L}} \\ I - V_{i}B_{e} \\ Q - V_{i}^{2}B_{e} \end{bmatrix}$$

$$(2.20)$$

where  $B_e$  is the total susceptance,  $\alpha$  is firing angle of thyristor,  $X_L$  is inductance,  $X_C$  is capacitance, I is injected current,  $V_i$  is terminal voltage of SVC. Equation (2.20) can be introduced into the power flow equation in the CPF process. It represents limits not only on the firing angle  $\alpha$ , but also on the current I, the control voltage V and the SVC voltage  $V_i$  as well as the reactive power Q.

### **2.3.2 STATCOM**

STATCOM is based on a solid state synchronous voltage source that is analogous to an ideal synchronous machine except the rotating part. It generates a balanced set of sinusoidal voltages at the fundamental frequency with rapidly controllable amplitude and phase angle. As shown in Figure 2.3, STATCOM is the voltage-source converter, which converts a DC input voltage into AC output voltage in order to compensate the active and reactive needed by the system. The reference signal  $Q_{ref}$  and  $P_{ref}$  can control the amplitude V and phase angle  $\beta$  of output voltage, respectively.

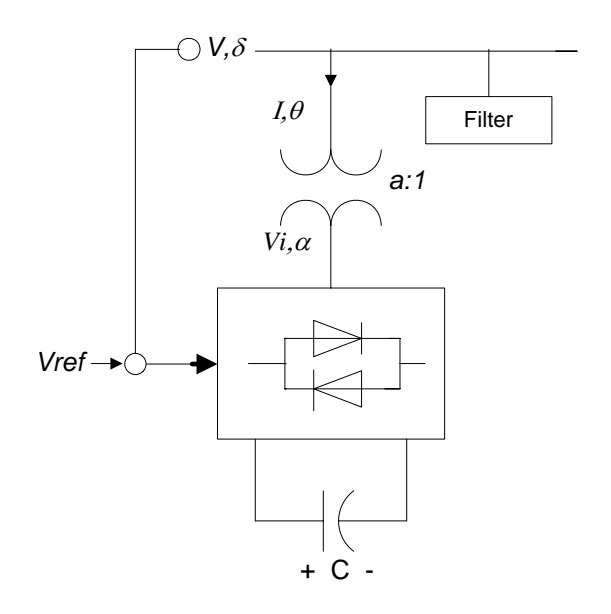


Figure 2.3: Basic structure of STATCOM.

Varying the amplitude of output voltage can control the reactive power exchange between STATCOM and the AC system. If the amplitude of the output voltage is increased above that of AC system voltage, STATCOM generates reactive power for the AC system. If the amplitude of the output voltage is decreased below that of the AC system, STATCOM absorbs the reactive power. If the output voltage is equal to the AC system voltage, the reactive power exchange is zero.

The real power exchanges between STATCOM and the AC system can be controlled by altering the phase angles between the inverter output and the AC system voltages. STATCOM supplies real power to the AC system if the output voltage is made to lead the corresponding AC system voltage. Conversely, STATCOM absorbs real power from the AC system, if the output voltage is made to lag the AC system voltage.

The process of energy transfer from the AC to DC side and vice versa in a voltage source converter is direct, i.e., the net instantaneous power at the AC terminals must always be equal to the net instantaneous power at the DC terminals, if the losses in the circuit are neglected. If a DC capacitor is connected across the input terminals of the converter, the converter keeps the DC capacitor voltage at a required level. The real power can be stored by making the converter output voltage lag the AC system voltage, so that the converter absorbs a small amount of real power from the AC system to cover its internal losses and keep the capacitor voltage at desired levels. The real power injected can be accomplished by making converter output voltage lead the AC system voltage. The ability to supply real power depends on the size of DC capacitor and the real power losses due to switching. However, large amount of real power injected can be accomplished by using other types of energy storage.

The STATCOM can provide both capacitive and inductive compensation and is able to control output current over the rated maximum capacitive or inductive range independent

of the AC system voltage. It can provide full capacitive output current at any practical system voltage when STATCOM is at the maximum limit. This is contrast to the SVC which can supply only diminishing output current with decreasing system voltage as determined by the designed maximum equivalent capacitive admittance. This type of controller is, therefore, more effective than the SVC in providing transmission voltage support and the expected stability improvements. In general, a reduction of more than 50 % in the physical size of installation can be expected when a STATCOM is compared to SVC. Also, for steady state reactive support, a STATCOM is capable of supporting higher loads than what would be possible with a SVC of comparable MVAr rating [11], [14].

There are two techniques for controlling the STATCOM. The first technique, referred to as phase control, is to control the phase shift  $\alpha$  to control the STATCOM output voltage magnitude. The other technique referred to as Pulse Width Modulation (PWM) on the other hand allows for independent control of output voltage magnitude and phase shift; in this case, the DC voltage is controlled separately from the AC output voltage.

The STATCOM increases voltage stability margin of the system by providing active and reactive power at the connected bus. Moreover, this device does not significantly alter the existing system impedance, which is an advantage over SVC.

In summary, STATCOM has better characteristics over SVC; when the system voltage drops enough to force the STATCOM output to ceiling, its maximum reactive power output will not affect by the voltage magnitude. Therefore, it exhibits constant current characteristics when the voltage is low under the limit. The steady state power exchange between the controller and the AC system is mostly reactive, as active power is only consumed to supply for the internal losses.

The p.u. DAEs corresponding to STATCOM controller are described as follows:

$$\begin{bmatrix} \dot{x}_c \\ \dot{\alpha} \\ \dot{m} \end{bmatrix} = f(X_c, \alpha, m, V, V_{dc}, V_{ref}, V_{dc, ref})$$
(2.21)

$$\dot{V}_{dc} = \frac{VI}{CV_{dc}}\cos(\delta - \theta) - \frac{1}{R_c C}V_{dc} - \frac{R}{C}\frac{I^2}{V_{dc}}$$
(2.22)

$$0 = \begin{bmatrix} P - VI \cos(\delta - \theta) \\ Q - VI \sin(\delta - \theta) \\ P - V^{2}G + kV_{dc}VG\cos(\delta - \alpha) + kV_{dc}VB\sin(\delta - \alpha) \\ Q + V^{2}B - kV_{dc}VB\cos(\delta - \alpha) + kV_{dc}VG\sin(\delta - \alpha) \end{bmatrix}$$

$$(2.23)$$

where  $V_{dc}$  is DC voltage of voltage source inverter, m is modulation index,  $\alpha$  is angle of internal synchronous source,  $R_c$  is internal DC losses due to switching,  $X_c$  is reactance of the capacitor,  $\delta$  is angle of voltage and  $\theta$  is angle of current.

The steady state model of STATCOM can be readily obtained from equations (2.21)-(2.23) as

$$0 = \begin{bmatrix} V - V_{ref} \pm X_{SL}I \\ V_{dc} - V_{dcref} \\ P - V_{dc}^2 / R_C - RI^2 \\ g(\alpha, k, V, V_{dc}, \delta, I, \theta, P, Q) \end{bmatrix}$$
(2.24)

Equation (2.24) includes AC and DC representation of STATCOM and it can be directly included in power flow program with the proper handling of limits, to analyze the static voltage stability of power system with STATCOM. If DC equations are introduced in the study, more practical solutions regarding to both AC and DC sides can be obtained.

### 2.3.3 TCSC

TCSC controllers use TCR in parallel with capacitor segments of series capacitor bank. The combination of TCR and capacitor allow the capacitive reactance to be smoothly controlled over a wide range and switched upon command to a condition where the bidirectional thyristor pairs conduct continuously and insert an inductive reactance into the line. The basic structure of the device is shown in Figures 2.4. The total susceptance of the line is controlled by controlling the firing angle of the thyristor.

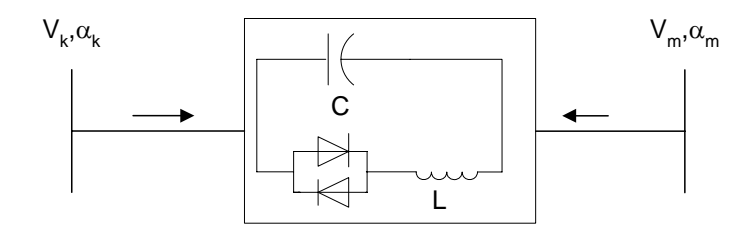


Figure 2.4: Basic structure of TCSC.

Suitable models to handle control limits and operation constraints are important. The p.u. DAEs corresponding to this device are shown as follows:

$$\begin{bmatrix} \dot{x}_c \\ \dot{\alpha} \end{bmatrix} = f(x_c, \alpha, V, V_{ref})$$
 (2.25)

$$0 = \begin{bmatrix} P + V_k V_m B_e \sin(\delta_k - \delta_m) \\ -V_k^2 B_e + V_k V_m B_e \cos(\delta_k - \delta_m) - Q_k \\ -V_m^2 B_e + V_k V_m B_e \cos(\delta_k - \delta_m) - Q_m \\ B_e - B_e(\alpha) \\ \sqrt{P^2 + Q_k^2} - IV_k \end{bmatrix}$$

$$(2.26)$$

where k and m are buses where TCSC is connected in between,

$$B_{e}(\alpha) = \pi \left(k_{x}^{4} - 2k_{x}^{2} + 1\right) \cos k_{x} (\pi - \alpha) /$$

$$\left\{X_{C} \left[\pi k_{x}^{4} \cos k_{x} (\pi - \alpha) - 2k_{x}^{4} \alpha \cos k_{x} (\pi - \alpha) + 2\alpha k_{x}^{2} \cos k_{x} (\pi - \alpha) - k_{x}^{4} \sin 2\alpha \cos k_{x} (\pi - \alpha) + k_{x}^{2} \sin 2\alpha \cos k_{x} (\pi - \alpha) - 4k_{x}^{3} \cos^{2} \alpha \sin k_{x} (\pi - \alpha) - 4k_{x}^{2} \cos \alpha \sin \alpha \cos k_{x} (\pi - \alpha)\right]\right\}$$

$$(2.27)$$

and

$$k_x = \sqrt{\frac{X_C}{X_L}} \tag{2.28}$$

The steady state model of TCSC can be easily obtained from (2.25)-(2.28) as

$$0 = \begin{bmatrix} B_e - B_{e,ref} \\ g(\alpha, V_k, V_m, \delta_k, \delta_m, I, P, Q_k, Q_m, B_e) \end{bmatrix}$$
(2.29)

which can be directly introduced into the power flow formulation. From equation (2.29), the total susceptance of TCSC can be controlled at a specific value.

#### 2.3.4 SSSC

SSSC is based on a solid-state synchronous voltage source employing an appropriate DC to AC inverter with gate turn-off thyristor, which can be used for series compensation of transmission lines. The SSSC is similar to the STATCOM as illustrated in Figure 2.5, as it is based on a DC capacitor fed VSI that generates a three-phase voltage at fundamental frequency, which is then injected in a transmission line through a transformer connected in series with the system.

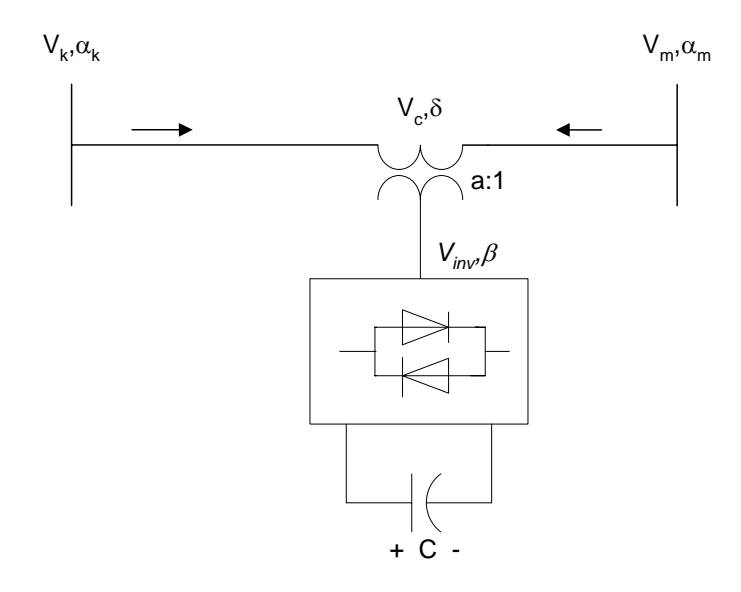


Figure 2.5: Basic structure of SSSC.

The main control objective of the SSSC is to directly control the current and indirectly the power, flowing through the line, by controlling the reactive power exchange between the SSSC and the AC system. The main advantage of this controller over a TCSC is that it does not significantly affect the impedance of the transmission system and, therefore, there is no danger of having resonance problem.

The p.u. DAEs of SSSC including the control and operation limits can be elaborated as follows:

$$\begin{bmatrix} \dot{x}_c \\ \dot{\beta} \\ \dot{m} \end{bmatrix} = f(x_c, \beta, m, I, V_{dc}, I_{ref}, V_{dcref})$$
(2.30)

$$\dot{V}_{dc} = \frac{VI}{CV_{dc}}\cos(\delta - \theta) - \frac{G_C}{C}V_{dc} - \frac{R}{C}\frac{I^2}{V_{dc}}$$
(2.31)

$$0 = \begin{bmatrix} P_k - V_k I \cos(\delta_k - \theta) \\ Q_k - V_k I \sin(\delta_k - \theta) \\ P_m - V_m I \cos(\delta_m - \theta) \\ Q_m - V_m I \sin(\delta_m - \theta) \\ P - P_k + P_m \\ Q - Q_k + Q_m \\ P - V^2 G + k V_{dc} V G \cos(\delta - \beta) + k V_{dc} V B \sin(\delta - \beta) \\ Q + V^2 B - k V_{dc} V B \cos(\delta - \beta) + k V_{dc} V G \sin(\delta - \beta) \end{bmatrix}$$

$$g(\beta, k, V_d, V_k, V_m, V, \delta_k, \delta_m, \delta, I, \theta, P_k, P_m, P, Q_k, Q_m, Q)$$

$$(2.32)$$

where  $\beta$  is angle of internal voltage,  $\delta$  is angle of AC voltage generated by SSSC,  $G_c$  is  $1/R_c$ .

To realize the models in power flow program, equations (2.30)-(2.32) are used as

$$0 = \begin{bmatrix} I - I_{ref} \\ V_{dc} - V_{dcref} \\ P - G_{c}V_{dc}^{2} - RI^{2} \\ g(\beta, k, V_{dc}, V_{k}, V_{m}, V, \delta_{k}, \delta_{m}, \delta, I, \theta, P_{k}, P_{m}, P, Q_{k}, Q_{m}, Q) \end{bmatrix}$$
(2.33)

which can be incorporated directly into the power flow program. DC equations are included in the formulation to provide more practical solutions regarding to DC side.

#### 2.3.5 **UPFC**

It is well known that UPFC is a versatile device for power flow control. The UPFC consists of two identical voltage-source inverters: one in shunt and the other one in series with the line; the general scheme is illustrated in Figure 2.6. Two inverters, namely shunt inverter and series inverter which operate via a common DC link with a DC storage capacitor, allow UPFC to independently control active and reactive power flows on the line as well as the bus voltage. Active power can freely flow in either direction between the AC terminals of the two inverters through the DC link. Although each inverter can generate or absorb reactive power at its own AC output terminal, they can not internally exchange reactive power through DC link. The VA rating of the injected voltage source is

determined by the product of the maximum injected voltage and the maximum line current at which power flow is still provided.

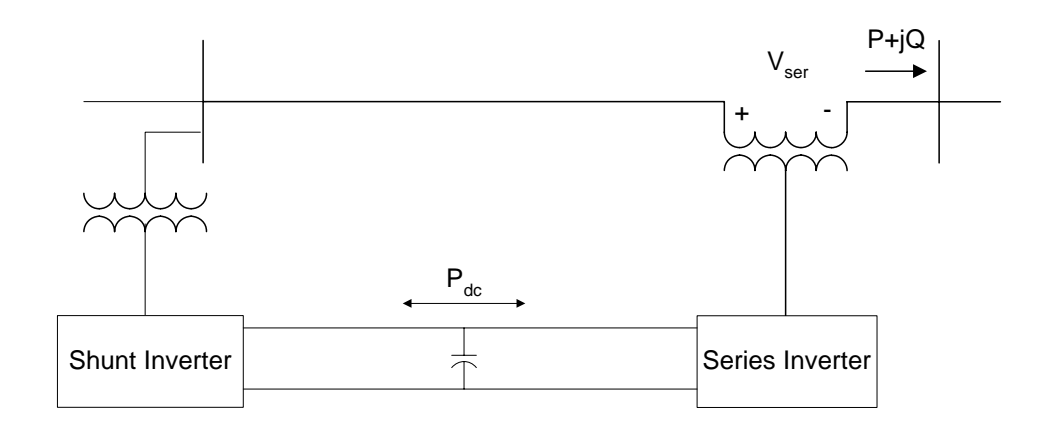


Figure 2.6: UPFC configuration.

The shunt inverter provides local bus voltage control when operated by itself as a STATCOM. When operated in conjunction with the series inverter, the shunt inverter has two functions: to control bus voltage by reactive power injection to the power system and to supply active power to the series inverter via the DC link for series flow control.

The series inverter, on the other hand, provides line power flow control by injecting an AC voltage with controllable magnitude and phase angle at the power frequency, in series with the line via an insertion transformer. This injected series voltage is, in effect, a synchronous series AC voltage source, which provides active series compensation for line voltage control and angle regulation through the transmission line current. The transmission line currents flow through this voltage sources resulting in active and reactive power exchange between the inverter and the AC system. The active power exchanged at the series AC terminal is converted by the inverter into DC power that appears at the DC link as positive or negative active power demand and transfer to the other converter located at the other side of the line.

It is obvious that the operation of UPFC is very important since it affects both the transmission line flow and voltage magnitude. Operation limit and control constraints of UPFC are very crucial to realize the actual operation of the device. To realize that, the validated p.u. DAEs corresponding to this model can be derived as follows:

$$\begin{bmatrix} \dot{x}_{c} \\ \dot{\alpha} \\ \dot{\beta} \\ \dot{m}_{sh} \\ \dot{m}_{se} \end{bmatrix} = f(x_{c}, \alpha, \beta, m_{sh}, m_{se}, V_{k}, V_{l}, V_{dc}, \delta_{k}, \delta_{l}, P_{l,ref}, Q_{l,ref}, V_{k,ref}, V_{dc,ref})$$

$$(2.34)$$

$$\dot{V}_{dc} = \frac{V_k I_{sh}}{C V_{dc}} \cos(\delta_k - \theta_{sh}) + \frac{V_m I_l}{C V_{dc}} \cos(\delta_m - \theta_l) 
- \frac{G_C}{C} V_{dc} - \frac{R_{sh}}{C} \frac{I_{sh}^2}{V_{dc}} - \frac{R_{se}}{C} \frac{I_l^2}{V_{dc}}$$
(2.35)

$$0 = \begin{bmatrix} P_{sh} - V_{k}I_{sh}\cos(\delta_{k} - \theta_{sh}) \\ Q_{sh} - V_{k}I_{sh}\sin(\delta_{k} - \theta_{sh}) \\ P_{sh} - V_{k}^{2}G_{sh} + k_{sh}V_{dc}V_{k}G_{sh}\cos(\delta_{k} - \alpha) + k_{sh}V_{dc}V_{k}B_{sh}\sin(\delta_{k} - \alpha) \\ Q_{sh} + V_{k}^{2}B_{sh} - k_{sh}V_{dc}V_{k}B_{sh}\cos(\delta_{k} - \alpha) + k_{sh}V_{dc}V_{k}G_{sh}\sin(\delta_{k} - \alpha) \end{bmatrix}$$

$$= \underbrace{\begin{bmatrix} P_{sh} - V_{k}I_{sh}\cos(\delta_{k} - \alpha) \\ P_{sh} - V_{k}I_{sh}\sin(\delta_{k} - \alpha) \end{bmatrix}}_{g_{sh}(\alpha, k_{sh}, V_{k}, V_{dc}, \delta_{k}, I_{sh}, \theta_{sh}, P_{sh}, Q_{sh})}$$

$$(2.36)$$

$$0 = \begin{bmatrix} P_{k} - P_{sh} - V_{k}I_{l}\cos(\delta_{k} - \theta_{l}) \\ Q_{k} - Q_{sh} - V_{k}I_{l}\sin(\delta_{k} - \theta_{l}) \\ P_{l} - V_{m}I_{l}\cos(\delta_{m} - \theta_{l}) \\ Q_{l} - V_{m}I_{l}\sin(\delta_{m} - \theta_{l}) \\ P_{k} - P_{l} - P_{sh} - P_{se} \\ Q_{k} - Q_{l} - Q_{sh} - Q_{se} \\ P_{se} - V^{2}G_{se} + k_{se}V_{dc}VG_{se}\cos(\delta - \beta) + k_{se}V_{dc}VB_{se}\sin(\delta - \beta) \\ Q_{se} + V^{2}B_{se} - k_{se}V_{dc}VB_{se}\cos(\delta - \beta) + k_{se}V_{dc}VG_{se}\sin(\delta - \beta) \end{bmatrix}$$

$$g_{se}(\beta, k_{se}, V_{dc}, V_{k}, V_{l}, V, \delta_{k}, \delta_{l}, \delta, I_{l}, \theta_{l}, P_{k}, P_{l}, P_{sh}, P_{se}, Q_{k}, Q_{l}, Q_{sh}, Q_{se})$$

$$(2.37)$$

$$0 = \begin{bmatrix} I_k \cos(\theta_k) - I_{sh} \cos(\theta_{sh}) - I_l \cos(\theta_l) \\ I_k \sin(\theta_k) - I_{sh} \sin(\theta_{sh}) - I_l \sin(\theta_l) \\ P_k - V_k I_k \cos(\delta_k - \theta_k) \\ Q_k - V_k I_k \sin(\delta_k - \theta_k) \end{bmatrix}$$

$$(2.38)$$

where *se*, *sh* represent series and shunt components, respectively and *l* represents the line used for current and power flow control.

The UPFC steady state model can be obtained by using the equations (2.34)-(2.38) as

$$0 = \begin{bmatrix} V_{k} - V_{k,ref} \\ V_{dc} - V_{dc,ref} \\ P_{se} - P_{se,ref} \\ Q_{se} - Q_{se,ref} \\ P_{sh} - P_{se} - G_{c}V_{dc}^{2} - R_{sh}I_{sh}^{2} - R_{se}I_{l}^{2} \\ g_{sh}(\alpha, k_{sh}, V_{k}, V_{dc}, \delta_{k}, I_{sh}, \theta_{sh}, P_{sh}, Q_{sh}) \\ g_{se}(\beta, k_{se}, V_{dc}, V_{k}, V_{l}, V, \delta_{k}, \delta_{l}, \delta, I_{l}, \theta_{l}, P_{k}, P_{l}, P_{sh}, P_{se}, Q_{k}, Q_{l}, Q_{sh}, Q_{se}) \\ g_{con}(V_{k}, \delta_{k}, I_{k}, I_{sh}, I_{l}, \theta_{k}, \theta_{sh}, \theta_{l}, P_{k}, Q_{k}) \end{bmatrix}$$

$$(2.39)$$

which again can be incorporated into the power flow program.

The limits of UPFC can be divided into 2 limits: shunt compensation limits and series compensation limit. Shunt compensation limits are basically firing angle and  $V_{dc}$  limits, which can be handled in the same way as the case of STATCOM. Series compensation limit, however, involves the capacity of the series compensation, which incorporates the active and reactive power limits.

### 2.4 Analysis Tools

In this study, voltage stability with FACTS devices are studied and validated with the help of a program developed in MATLAB and standard CPF program, UWPFLOW. UWPLOW is a research tool that has been designed to calculate maximum loading margin of the power system associated with saddle-node and limit-induced bifurcation for given load and generation directions [59]. The program has detailed static models of various power system elements such as generators, loads, HVDC links, and various FACTS controllers, particularly SVC, STATCOM and TCSC devices under phase and PWM control schemes, representing control limits with accuracy of for all models. There are no models for SSSC and UPFC controllers available in UWPFLOW. Programs developed in MATLAB are used to find the solution of voltage stability study with FACTS devices. The result developed in MATLB is compared with UWPFLOW for the case of SVC, STATCOM and TCSC.

## 2.5 Test Systems

### 2.5.1 IEEE 14-bus Test System

The IEEE 14-bus test system is used to test the proposed method. A single line diagram of the IEEE 14 bus test system is depicted in Figure 2.7, which consists of five synchronous machines, including three synchronous compensator used only for reactive power support and two generators located at buses 1 and 2 [11]. In the system, there are twenty branches and fourteen buses with eleven loads totaling 259 MW and 81.4 Mvar. The value of 259 MW is used as the base MVA in the IEEE 14-bus test system.

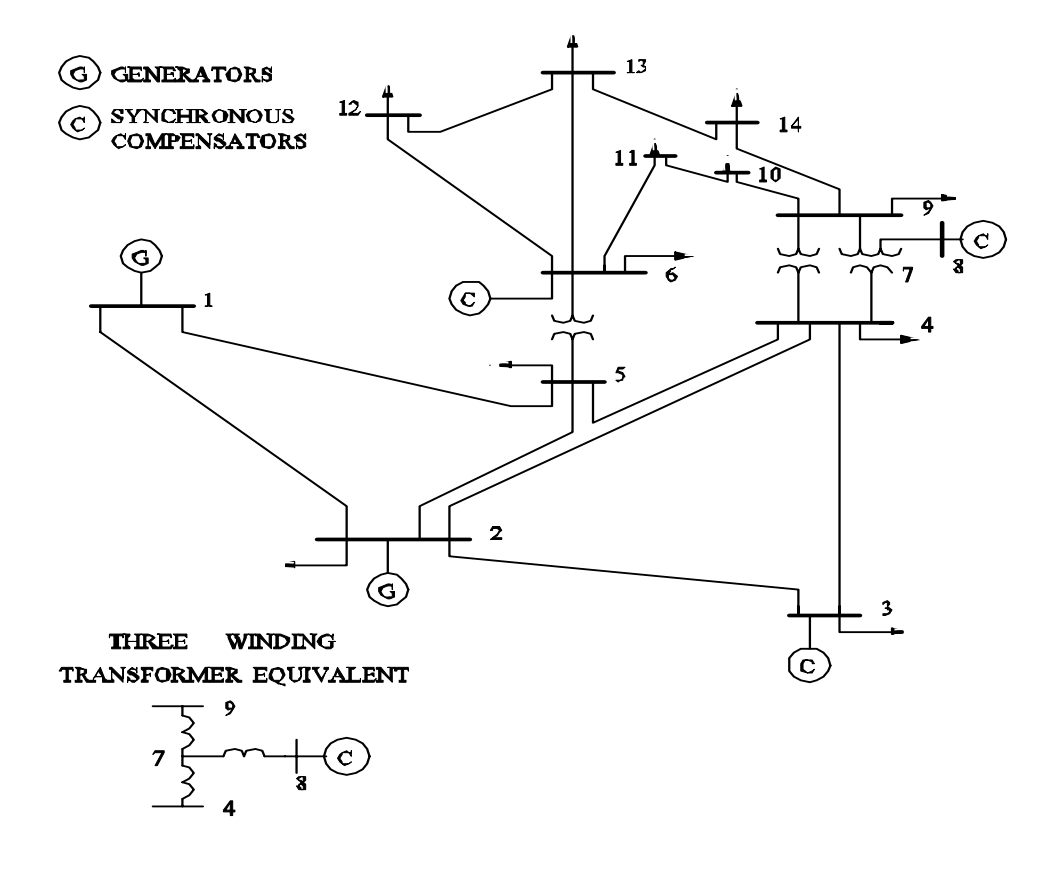


Figure 2.7: Single line diagram of the IEEE 14 bus system.

### 2.5.2 Modified IEEE 14-bus Test System

A single line diagram of the modified IEEE 14 bus test system is depicted in Figure 2.8, which consists of five synchronous machines, including one synchronous compensator used only for reactive power support. These synchronous generators are located at buses 1, 2, 6 and 8. The modification from the original IEEE 14-bus test system is that generators located at buses 6 and 8 were changed from synchronous compensators to generators.

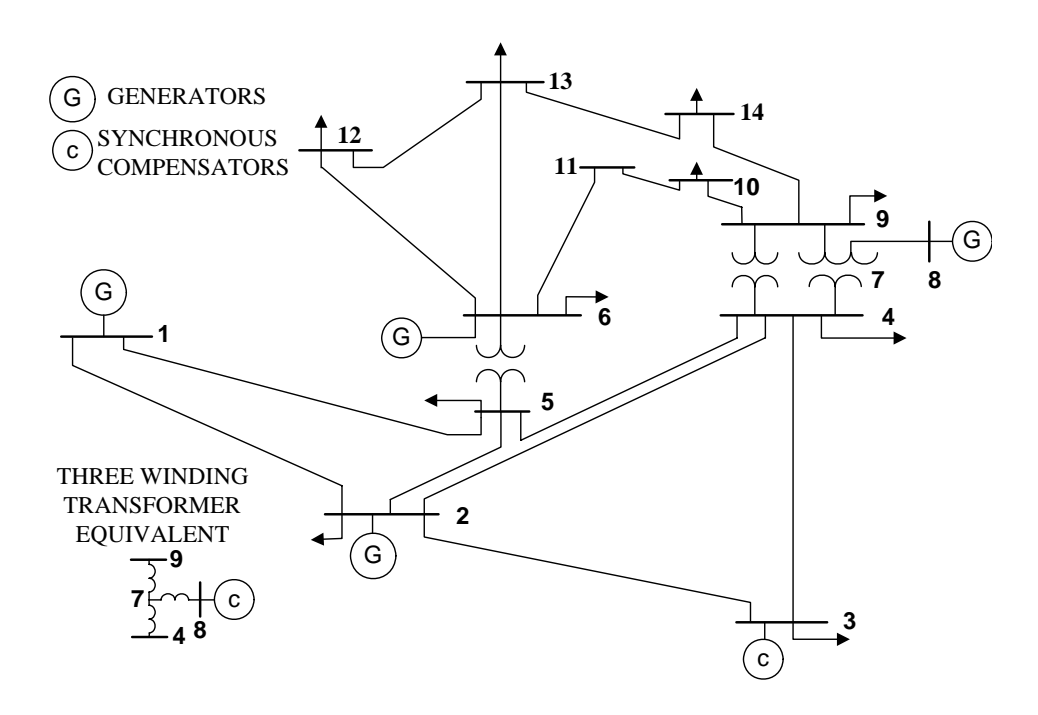


Figure 2.8: Single line diagram of the modified IEEE 14 bus system.

### 2.6 Summary

This chapter presents concepts and analysis techniques for voltage stability study in power systems. Various ways to enhance voltage stability margin including an introduction of FACTS devices are also presented in the chapter. Equations representing AC and DC parts of well-known FACTS devices are presented and they can be introduced directly into load flow equations in static voltage stability study. Analysis tools and test systems used throughout the study for voltage stability with FACTS devices are also presented.

## Chapter 3

#### INFLUENCE OF FACTS CONTROLLERS

#### 3.1 Introduction

In power system, installation of FACTS controllers, which are power-electronics-based devices designed for the direct control of AC transmission systems, is completely changing the way transmission system controlled and operated. They are mainly used to increase stability of power systems. FACTS controllers can modify the power system structure by delivering/absorbing active and/or reactive power at the connected location. FACTS devices are presented in terms of the two key benefits, namely to extend power transfer limit and to provide better control of flow on parallel paths. The former is generally more important in regions with long distance to load, while the latter is more important in relatively tight mesh networks.

According to the connection, FACTS devices can be divided into three categories, namely shunt, series and shunt-series FATCS devices. In this chapter, voltage stability assessment and enhancement of various FACTS devices are studied and compared based on their connection. In the first part, voltage stability assessment and enhancement of shunt FACTS devices are investigated and compared in the modified IEEE 14-bus test system. In the second part, series FACTS devices and UPFC are investigated in the same test system. All FACTS devices are compared and discussed in the final part to see the relative usefulness of each type of FACTS devices regarding static voltage stability margin enhancement.

This chapter is organized as follows: Section 3.2 presents voltage stability assessment and enhancement of shunt FACTS devices. In Section 3.3, series FACTS devices and UPFC are studied for voltage stability assessment/enhancement. All FACTS devices are then compared and discussed in Section 3.4. Finally, in Section 3.5, a summary, discussion and contribution are given.

#### 3.2 Shunt FACTS Controllers

Voltage stability assessment with shunt FACTS devices, namely SVC and STATCOM, is carried out and compared in this section. Firstly, placements and sizing issues of shunt FACTS devices are investigated according to static voltage stability in static time frame. Then, voltage stability assessment and enhancement are investigated and compared in terms of PV curves, LM, voltage profiles, losses and contingencies.

#### 3.2.1 Placement

The best location for reactive power compensation for improving static voltage stability margin is the "weakest bus" of the system [11],[15],[17]. Weakest bus is defined as the one that is nearest to experiencing voltage collapse. The weakest bus of the system can be identified by using tangent vector analysis [11],[34]. Table 3.1 shows the first four weakest buses of IEEE 14-bus test system i.e. buses having highest magnitudes of tangent vectors. From Table 3.1, the bus 14 could be considered as the best location for a reactive power support, as the absolute value of tangent vector or the change of voltage is highest at this bus. Introducing shunt FACTS device at this location will improve voltage stability margin the most.

Table 3.1: Tangent vector of the first four weakest buses

Bus No	Tang. Vectors
14	0.015802
10	0.01404
13	0.013938
9	0.013764

#### 3.2.2 Suitable Size

In order to get a rough estimate of reactive power support needed at the weakest bus and corresponding loading margin for a given load and generation direction, a synchronous compensator with no limit on reactive power was used at the weakest bus. The amount of reactive generated at the maximum loading point from the synchronous compensator was found to be 150 MVAr at 1.0 p.u. voltage. This will be a good starting point of shunt FACTS capacities.

Another method of determining the capacities is to find the relationship between the maximum Loading Factor and the corresponding capacities that the devices can deliver without having the voltage collapse. These relationships for SVC and STATCOM are given in Figure 3.1. Voltage control is used for SVC and STATCOM. The voltage setting of these devices is 1.0 p.u.

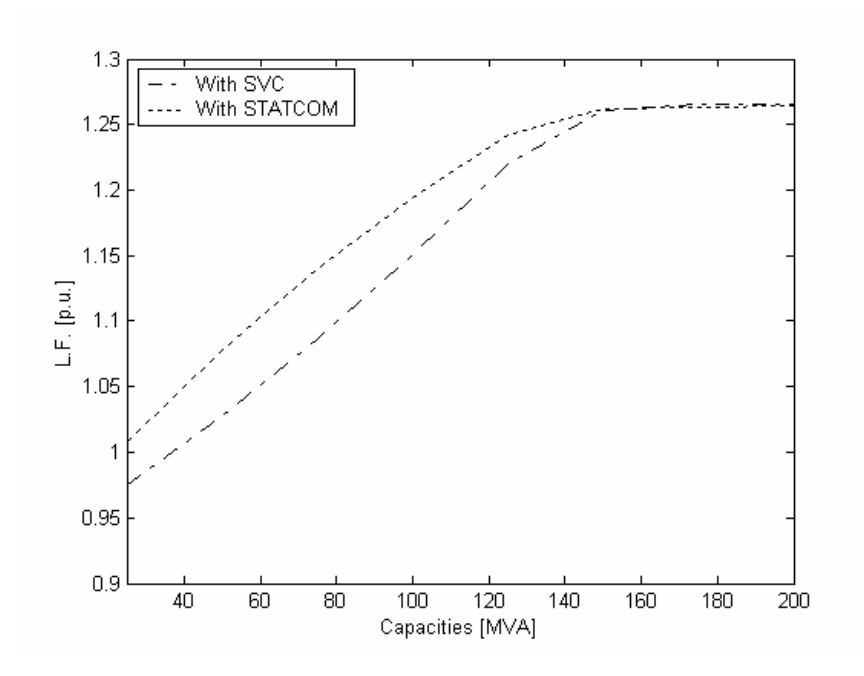


Figure 3.1: Loading margin vs controller capacities for shunt controllers.

It is clear from Figure 3.1, the optimum capacity required for both SVC and STATCOM is 150 MVAr, same as the value obtained from the synchronous compensator study. Beyond this capacity there is no improvement in the loading margin. As the results of two methods, the capacity of  $\pm 150$  MVAr will be used as the maximum reactive power capacity for SVC and STATCOM. Negative size of shunt FACTS devices is chosen to be equal to positive size as it happens in many shunt FACTS devices. However, it is not used in static voltage stability study as the reactive power demand is always increasing.

#### 3.2.3 PV Curves and Voltage Profiles

PV curves at the weakest bus for base case, with shunt FACTS device are given in Figure 3.2. In the base case, the voltage is dropped dramatically into unacceptable value (0.9 p.u.) beyond the LF value of 0.6 p.u. and collapses at LF = 0.92 p.u. As can be seen from the P-V curves, shunt FACTS devices improve the static voltage stability margin of the system by moving the nose point of P-V curve out. This also makes the voltage magnitude at the weakest bus in the acceptable range even for a higher loading point. Table 3.2 shows LM and percent increase of LM for base case and system with SVC and STATCOM. From the table, SVC increases LM of the system up to 36% higher than that of the base case. Compared with STATCOM, SVC provides a close value of LM, since it is operated within the limit. A snapshot of voltage profiles close to the collapse point at all the buses of the base case and with different shunt FACTS controllers are given in Figure 3.3. Notice that SVC and STATCOM provide a good overall voltage profile with higher LM compared to the base case.

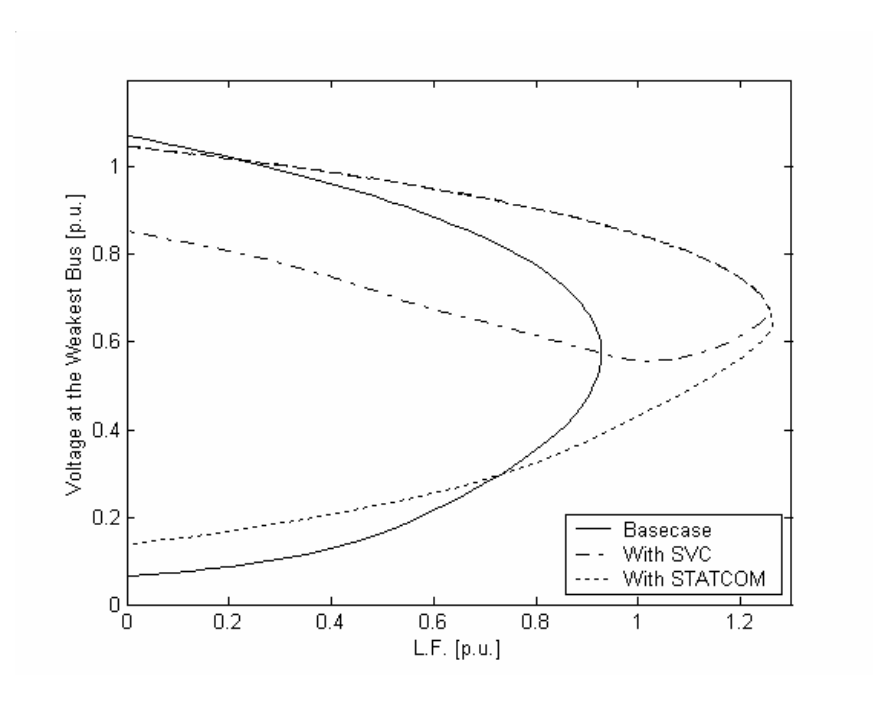


Figure 3.2: PV curves of Base case, with various shunt FACTS controllers.

Table 3.2: LM and % Increase of LM for base case, with SVC and STATCOM

Case	Loading Margin [p.u]	% Increase of LM from base case
Base Case	0.9278	-
SVC	1.2606	35.9
STATCOM	1.2625	36.1

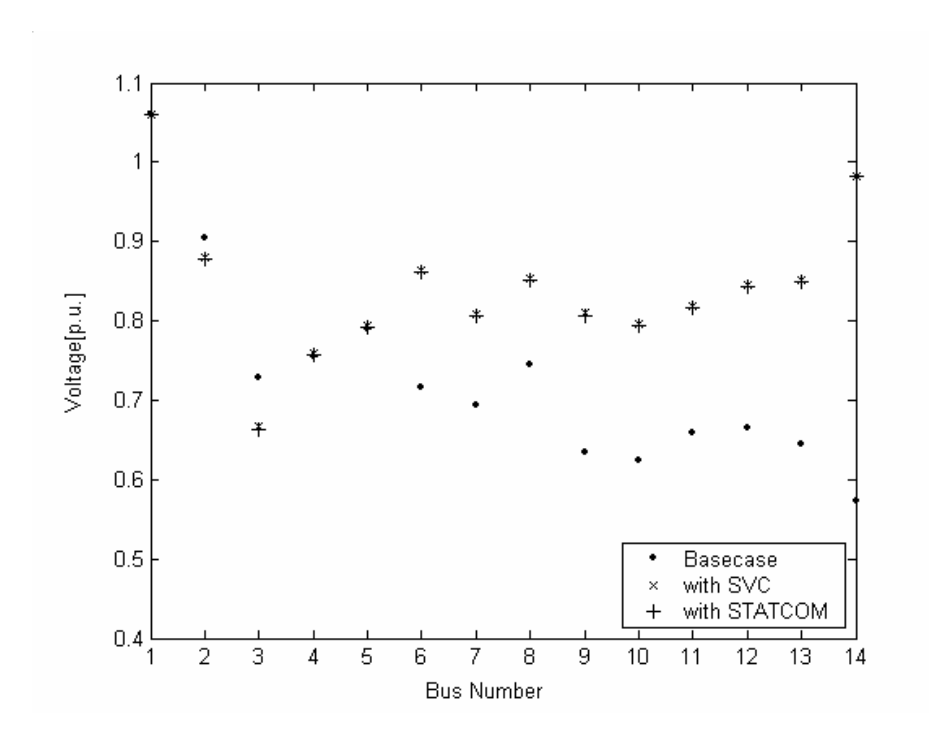


Figure 3.3: Voltage Profiles of each bus at LM for Base case and different controllers.

#### 3.2.4 Power Losses

In exploring the benefits of these FACTS controllers, the real and reactive power losses in the system at various loading levels are calculated and compared with those of the base case.

Active and reactive power losses in the system at different loading points for base case and different controllers are given in Figures 3.4 and 3.5, respectively. The real and reactive power losses appear to be following the same pattern in this test system. Notice that at the higher loading factor, both real and reactive power losses increase very rapidly. There is not significant improvement in the loss reduction with SVC and STATCOM at the lightly loaded conditions up to L.F.=0.4 p.u. However, a substantial amount of reduction in the losses is achieved at the higher loaded conditions.

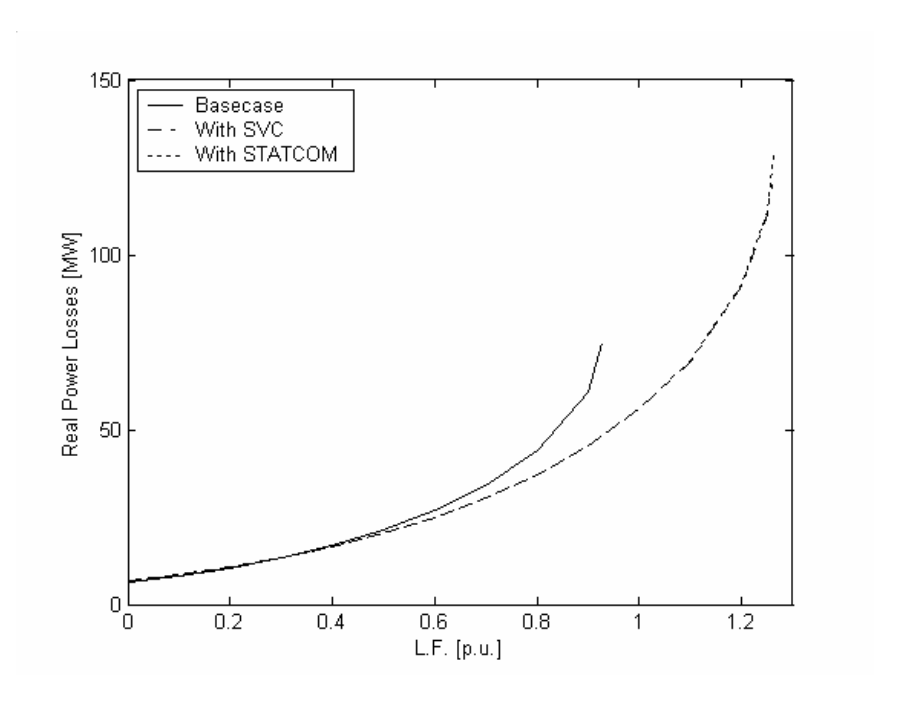


Figure 3.4: Real power losses in the system for different shunt controllers.

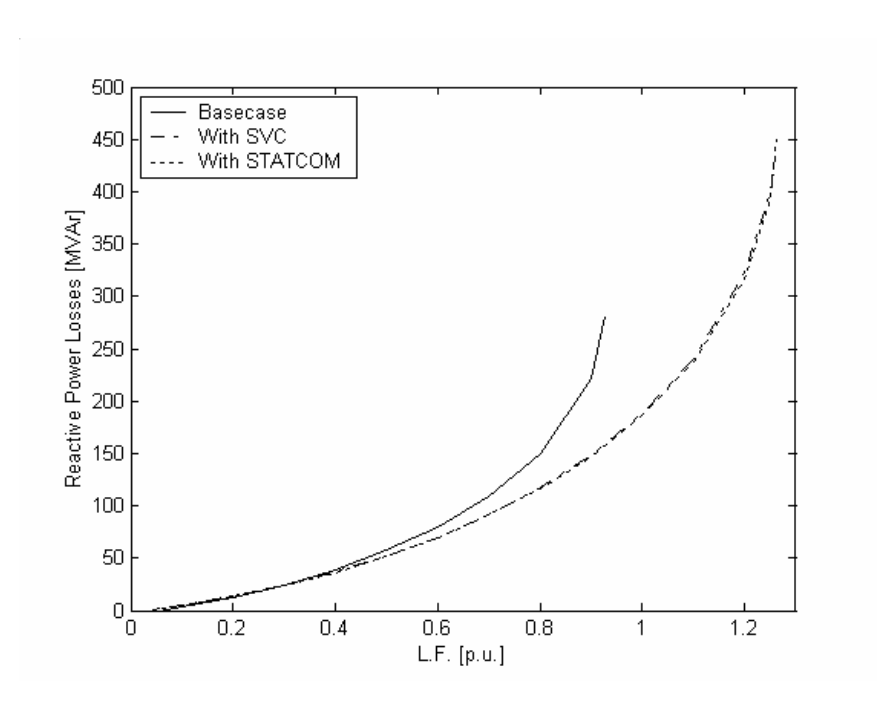


Figure 3.5: Reactive power losses in the system for different shunt controllers.

#### 3.2.5 Contingency

In case of contingencies, the system characteristics have changed. The first three most severe contingencies of the system are found by determining loading margin of the system after contingency. The outages of line 1-2, 2-3 and 1-5 are the first three severe cases in the system. The system behaves like a radial system since most of the generation are generated at buses 1 and 2. The lines adjacent to generators have to carry heavy load and trend to have most severity for the outages. The maximum loading margins in each outage are given in Table 3.3 for different cases. From Table 3.3, the most severe contingency in the system is the outage of line 1-2, which has the lowest LM. With SVC or STATCOM, LM can be increased for all contingency cases. SVC provides close value of LM compared to STATCOM.

Table 3.3: Loading Margin for various line outages for base case and different controllers

Case	Loading Margins [p.u.] for line outages			
	1-2	2-3	1-5	
Base Case	0.25184	0.38278	0.59605	
SVC	0.40205	0.49212	0.87061	
STATCOM	0.40097	0.49174	0.86916	

#### 3.3 Series FACTS Controllers and UPFC

Voltage stability assessment with series FACTS devices and UPFC are studied in this section. At first, placement and sizing issues of these FACTS devices are presented. Then, voltage stability assessment, including PV curves, voltage profiles, losses and contingency are carried out and presented.

Current control mode is used for TCSC, SSSC and UPFC devices. The current at a specific line is controlled at 0.0943 p.u., which corresponds to the power flow of 0.1 p.u. With this current value, solutions can be obtainable at most of the cases. For STATCOM and shunt part of UPFC, the voltage magnitude is controlled at 1.0 p.u. It is noted that current and voltage can be controlled at other values if the solution is obtainable.

#### 3.3.1 Placement

### Series Compensation devices

Reactive-power loss sensitivity approach is proposed to narrow down the candidates and to identify the weakest line of the system. The weakest line is defined as a line that needs the reactive power the most. If the series compensation device is introduced at this line, the loading margin of the system will be increased to the maximum value. Reactive power loss sensitivity can be found by the ratio of the change of reactive power losses and the load increase. To validate the methodology and possibility to the power system applications, some simulations have been conducted in the test system under various system conditions including stressed system conditions, which consider N-1 contingency in a transmission line.

To verify the effectiveness of the proposed method, the results of line ranking according to reactive power loss sensitivity ( $\partial Q_{loss}/\partial \lambda$ ) for the IEEE 14-bus system and the modified IEEE 14-bus test system are shown in Tables 3.4 and 3.5 for the cases of normal condition and N-1 contingency at line 2-3, respectively. From the results, it can be noticed that lines 1-5 and 1-2 require the reactive power compensation the most, as it has the highest  $\partial Q_{loss}/\partial \lambda$ . Having TCSC connected in lines 1-5 or 1-2 would increase loading margin to the maximum amount compared to other cases. Connecting TCSC at line 3-4 in case of N-1 contingency at line 2-3 would result in the maximum loading margin.

The sensitivity index is computed at the collapse point. The compensation device is located based on the sensitivity index, which identifies the location needing reactive power the most. The sensitivity index is sensitive to contingencies, as the power system network is changed when contingency is occurred. The criterion for the use of sensitivity index depend upon operating condition i.e. normal or contingency conditions defined by utilities. If the contingency is occurred at FACTS devices, the worst situation may be occurred. In this study, N-1 contingency of FACTS devices is neglected.

Table 3.4: Tie Line Index near LM of IEEE 14 bus test systems in normal condition

Line	$\partial Q_{ m loss}/\partial \lambda$			
Line	IEEE 14-bus test system	Modified IEEE 14-bus test system		
1-2	2.430 (2)	6.177 (1)		
1-5	2.480 (1)	5.495 (2)		
2-3	1.750 (3)	4.922 (3)		
2-4	1.170 (4)	2.434 (4)		
2-5	0.730 (5)	1.385 (5)		
3-4	0.190 (7)	0.789 (6)		

Table 3.5: Tie Line Index near LM of IEEE 14 bus test systems with N-1 (Line 2-3)

Line	$\partial Q_{ m loss}/\partial \lambda$			
Line	IEEE 14-bus test system	Modified IEEE 14-bus test system		
1-2	0.440 (4)	1.041 (4)		
1-5	0.800 (2)	1.810 (2)		
2-4	0.670 (3)	1.626 (3)		
2-5	0.360 (5)	0.813 (5)		
3-4	1.120 (1)	4.484 (1)		
4-5	0.210 (6)	0.640 (6)		

The results obtained in base case without TCSC and cases having TCSC connected at specific lines in base case and N-1 contingency in test systems are tabulated in Table 3.6. From Table 3.6, it is obvious that the reactive-power loss sensitivity method offers close results in ranking the lines in terms of weakness compared to the case with TCSC both in normal and in contingency conditions. However, in the modified IEEE 14-bus test system, there is one incorrect ranking in the first position in the normal case due to close values of LM. However, a group of candidate buses having high reactive-power loss sensitivity could be considered. According to this, the reactive power sensitivity method provides an effective method not only to identify the weakest bus but also to rank the lines in terms of reactive power losses. Since TCSC at line 1-5 increases the loading margin the most in normal condition, in the rest of the study, the series FACTS devices are placed at line 1-5.

Table 3.6: Loading Margin of Base case and system with TCSC connected

T C	Loading Margin [p.u.]				
Location of TCSC	IEEE 14-bus te	est system	st system Modified IEEE 14-bus tes		
	Normal	N-1	Normal	N-1	
No TCSC	0.70398	0.24292	0.9278	0.4403	
Line 1-2	0.93501 (2)	0.32999 (4)	0.9437 (4)	0.4406 (4)	
Line 1-5	1.0052 (1)	0.40591 (2)	0.9579 (1)	0.5106 (2)	
Line 2-4	0.84004 (3)	-	0.9468 (2)	-	
Line 2-5	0.75681 (4)	0.33042 (3)	0.9455 (3)	0.4485 (3)	
Line 3-4	0.73623 (5)	0.29126 (6)	0.9415 (5)	0.4093 (6)	
Line 4-5	0.71908 (8)	0.45186 (1)	0.9231 (6)	0.6490 (1)	

#### **UPFC**

The best location for introducing UPFC controller can be found from a group of candidate locations of shunt and series compensation devices, which presented in Tables 3.1 and 3.6, respectively. From the group of candidate buses, it was found that, for the modified IEEE 14-bus test system, UPFC should be placed at line 9-14 to have the highest LM. Line 9-14 is one of candidate locations of shunt FACTS device as it is the line connected to the weakest bus, bus 14.

#### 3.3.2 Suitable Size

Series Compensation devices

Sizing of TCSC and SSSC can be found from voltage stability study. The size of these series devices can be found by plotting the corresponding capacity of these devices against various loading factors. For TCSC, Figure 3.6 shows the capacity of  $Q_k$ -reactive power delivered at the sending bus,  $Q_m$ -reactive power absorbed at the receiving bus and Q-reactive power delivered/absorbed by TCSC with respect to loading factors. From the Figure 3.6, the reactive capacity of TCSC is about 2.4 MVAr at the collapse point. Hence, the value of 2.4 MVAr is used as the capacity of TCSC. In the base case, real and reactive power flow in line 1-5 are 0.3838 and 0.05 p.u., respectively.

Figures 3.7 and 3.8 show the corresponding active and reactive power capacities of SSSC at various load factors. From Figures 3.7 and 3.8, it is noticed that active and reactive

power exchanges of SSSC are 0.2 MW and 12.5 MVAr, respectively. These values are used for the active and reactive power capacity of SSSC.

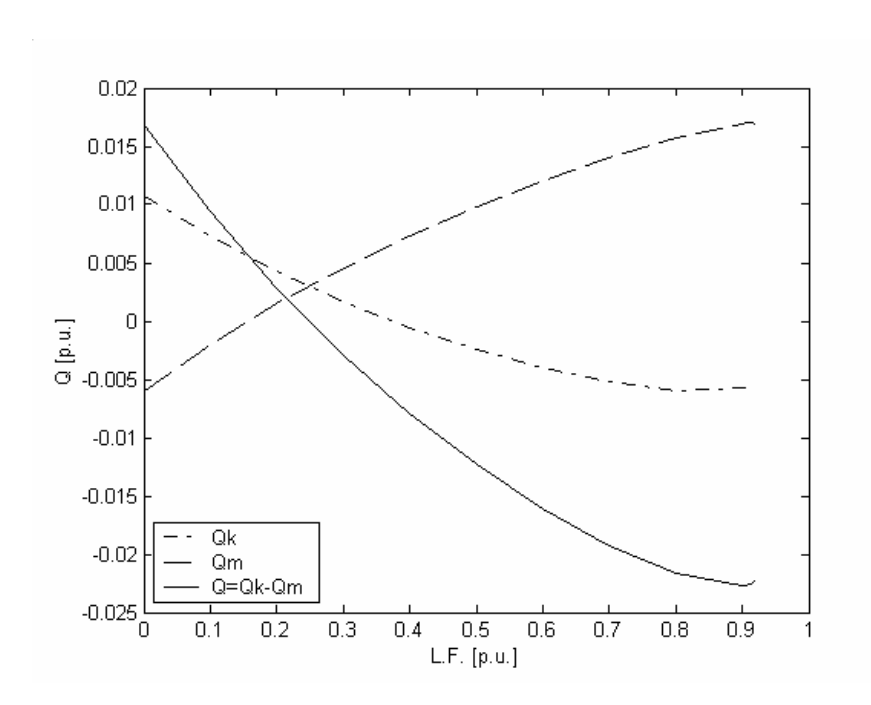


Figure 3.6: Capacity of TCSC at various LFs.

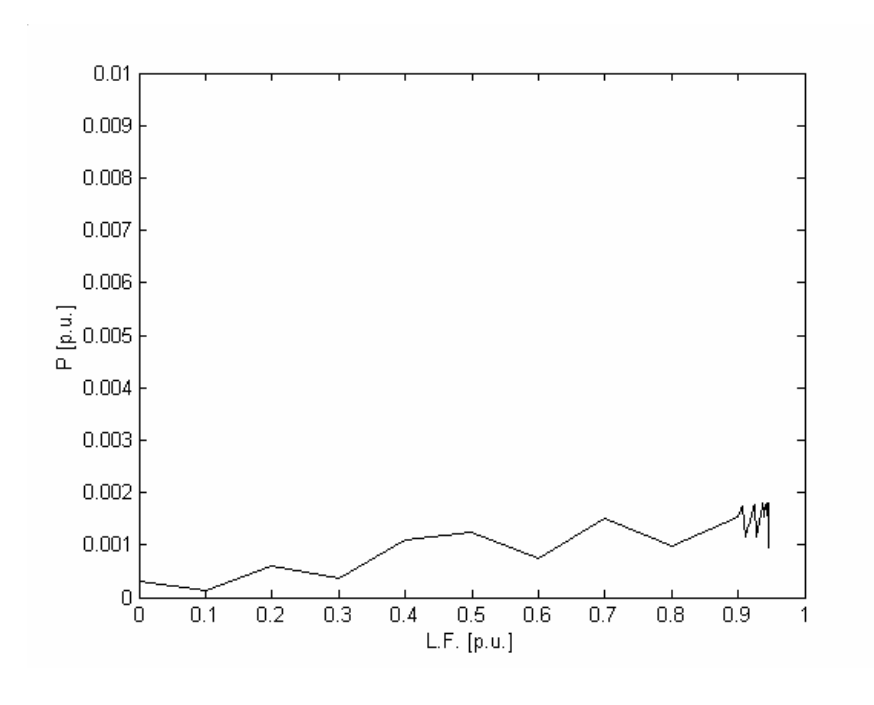


Figure 3.7: Active power capacity of SSSC at various LFs.

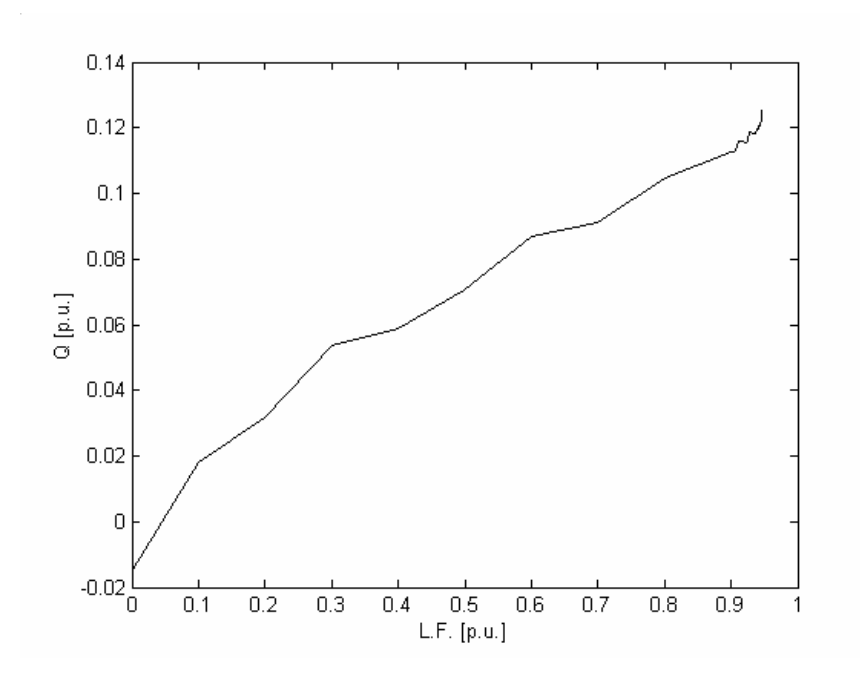


Figure 3.8: Reactive power capacity of SSSC at various LFs.

#### UPFC

The capacity of UPFC can be also found from the active and reactive power needed by the devices at the collapse point. The capacities of shunt and series component are plotted separately. Figures 3.9 and 3.10 show the plots of active power required by series and shunt components of UPFC, respectively. From Figures 3.9 and 3.10, active power required for series and shunt components are 0.45 and 2.3 MW, respectively. Figure 3.11 and 3.12 show reactive power needed by series and shunt components of UPFC, respectively. From Figures 3.14 and 3.15, it can be seen that reactive power requirement are 18.4 and 100 MVAr for series and shunt components, respectively. The capacity of UPFC is much lower than that of STATCOM, which is 150 MVAr. With these capacities, UPFC gives a loading margin of 1.4165 p.u. In practice, the parameters of FACTS devices including capacities, reactance, etc. should be selected based on practical values. Notice from Figures 3.7, 3.9 and 3.10 that numerical oscillation is due to small values of real power.

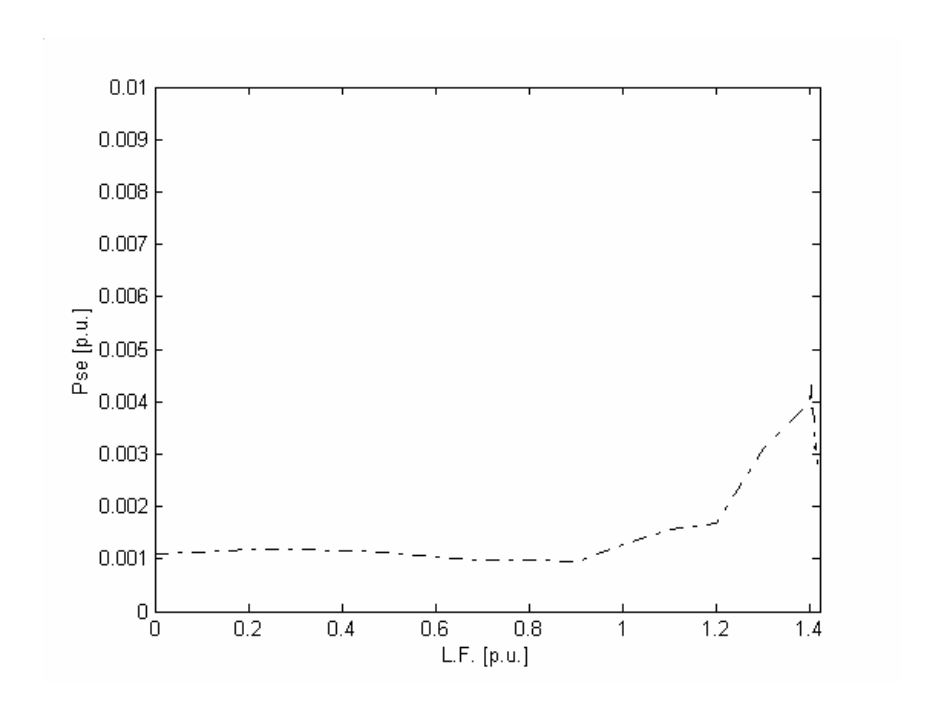


Figure 3.9:  $P_{se}$  of UPFC at various LFs.

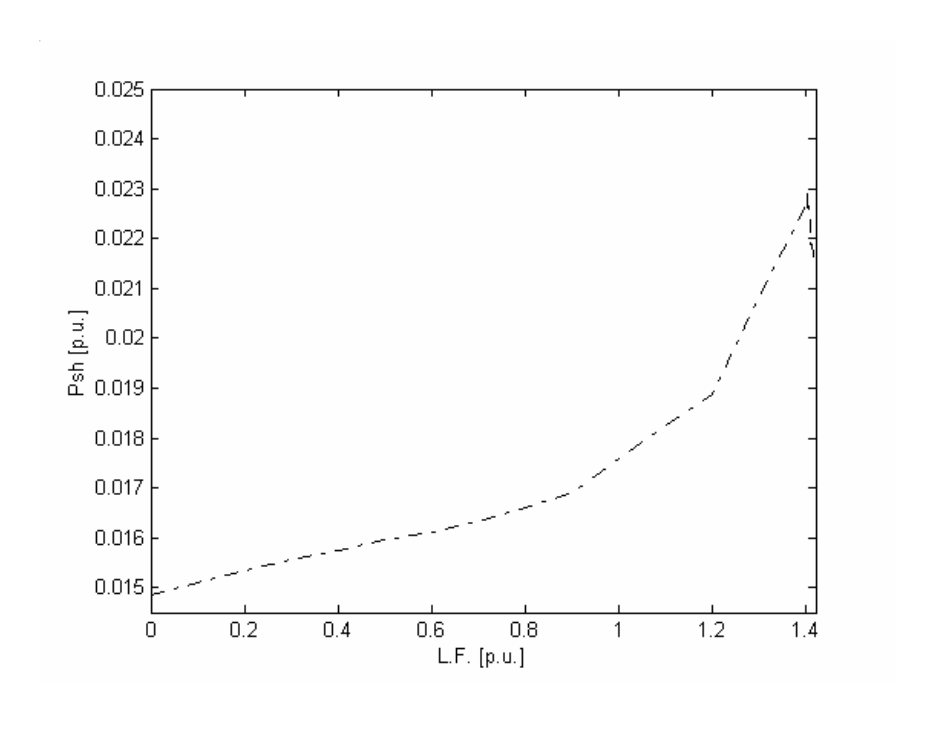


Figure 3.10:  $P_{sh}$  of UPFC at various LFs.

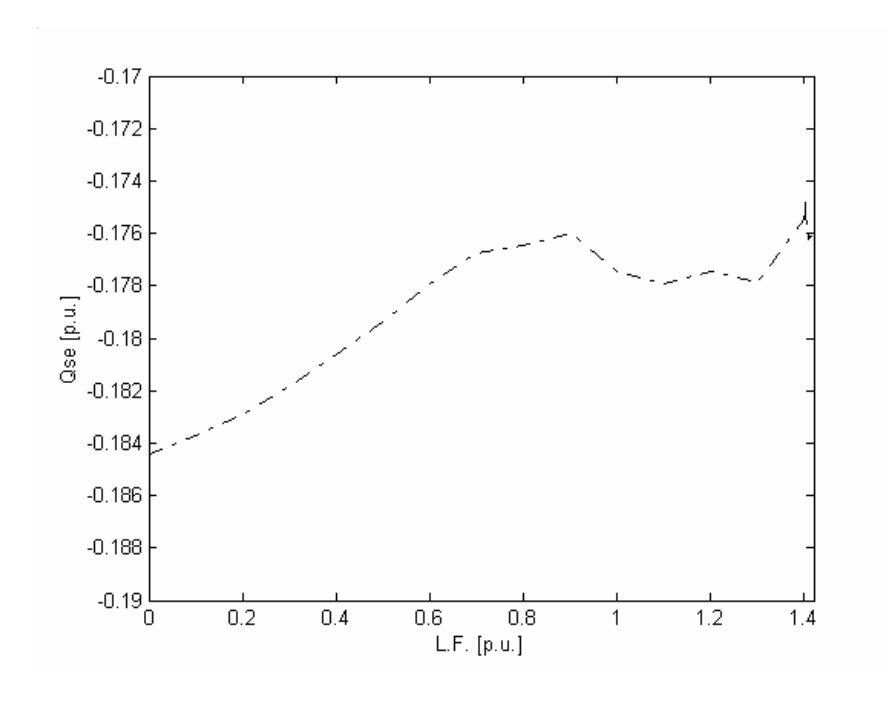


Figure 3.11:  $Q_{se}$  of UPFC at various LFs.

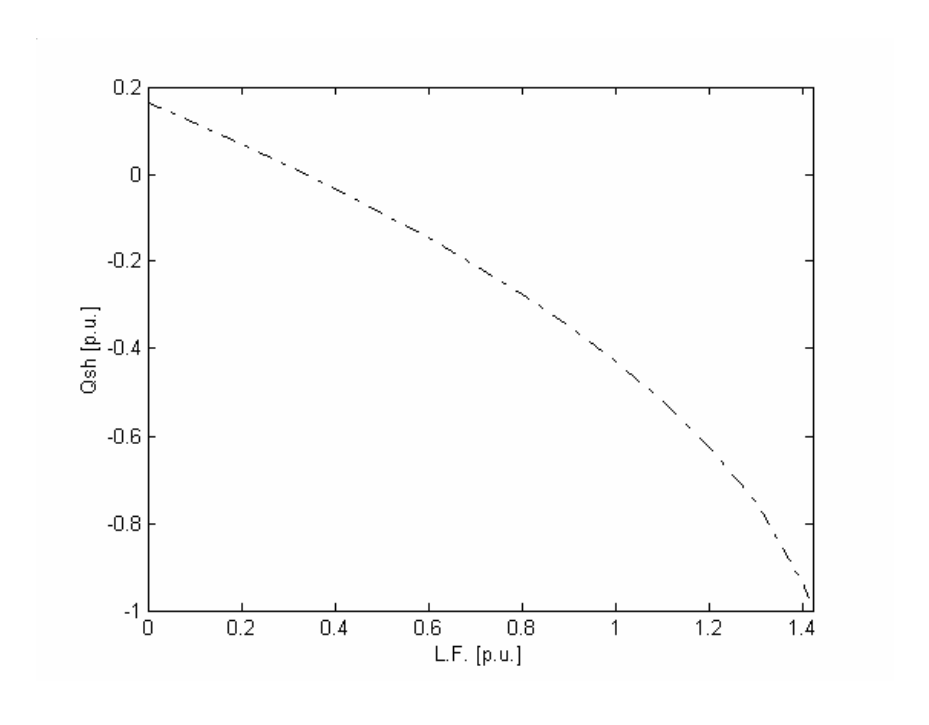


Figure 3.12:  $Q_{\text{sh}}$  of UPFC at various LFs.

### 3.3.3 PV Curves and Voltage Profiles

PV curves of base case without FACTS and with series FACTS devices are shown in Figure 3.13. The loading margin of the system is increased slightly with the help of the series devices, much lower than that of shunt devices. SSSC gives a slightly higher LM than TCSC since SSSC delivers both active and reactive power. Also, the reactive capacity of SSSC is higher than that of TCSC.

Figure 3.14 compares PV curves of without (base case) and with UPFC. Obviously, from the figure, the LM of the system with UPFC is much higher than that of the base case. The values of loading margins with series FACTS devices and UPFC are compared in Table 3.7. From Table 3.7, it is obvious that UPFC gives the highest LM compared to other devices. Series FACTS devices give much lower LM than shunt FACTS devices. This is due to the reason that the weakest bus (bus 14) requires reactive power the most and it is situated in the distribution level, far away from the source. Introducing reactive power support at the connected line is not an efficient way to increase voltage stability margin in the IEEE 14-bus test system.

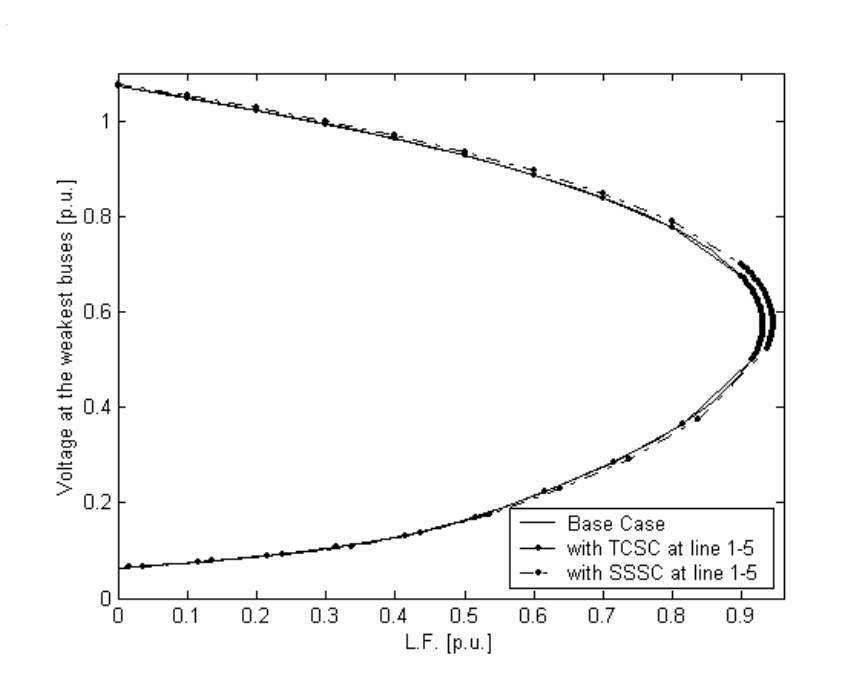


Figure 3.13: PV curves of base case. with TCSC and SSSC at line 1-5.

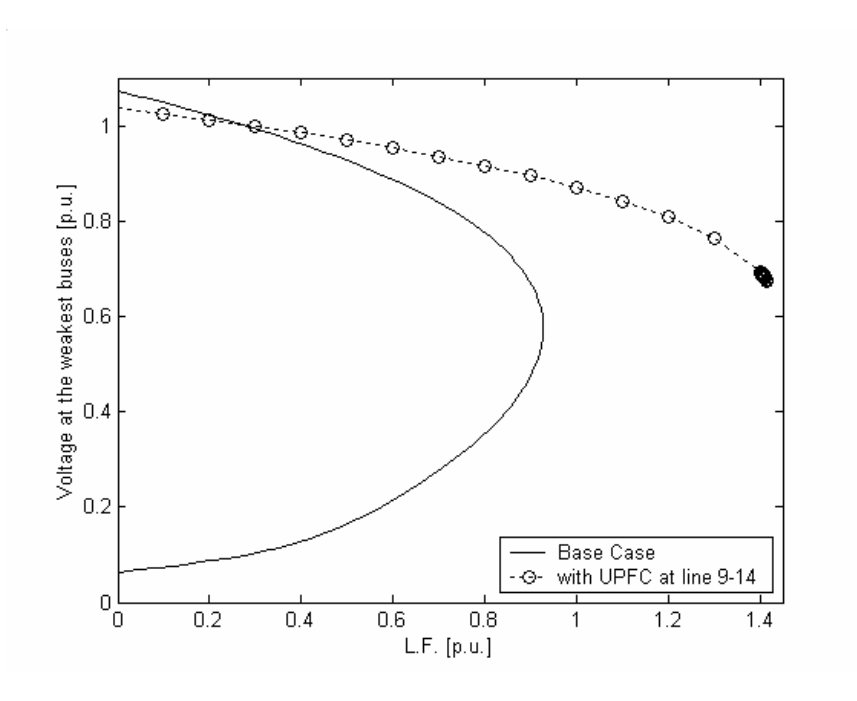


Figure 3.14: PV curves of base case, with UPFC at line 9-14.

Table 3.7: Loading Margin and % Increase of LM of base case and system with TCSC, SSSC and UPFC.

Case	Loading Margin [p.u]	% Increase of LM from base case
Base Case	0.9278	-
TCSC	0.9307	0.3
SSSC	0.9452	1.9
UPFC	1.4165	52.7

Voltage profiles at the collapse point of base case and system with TCSC, SSSC and UPFC are shown in Figure 3.15. Notice from Figure 3.15 that UPFC gives better overall voltage profiles compare to TCSC and SSSC. This is because UPFC provide both real and reactive power support in shunt and series connections.

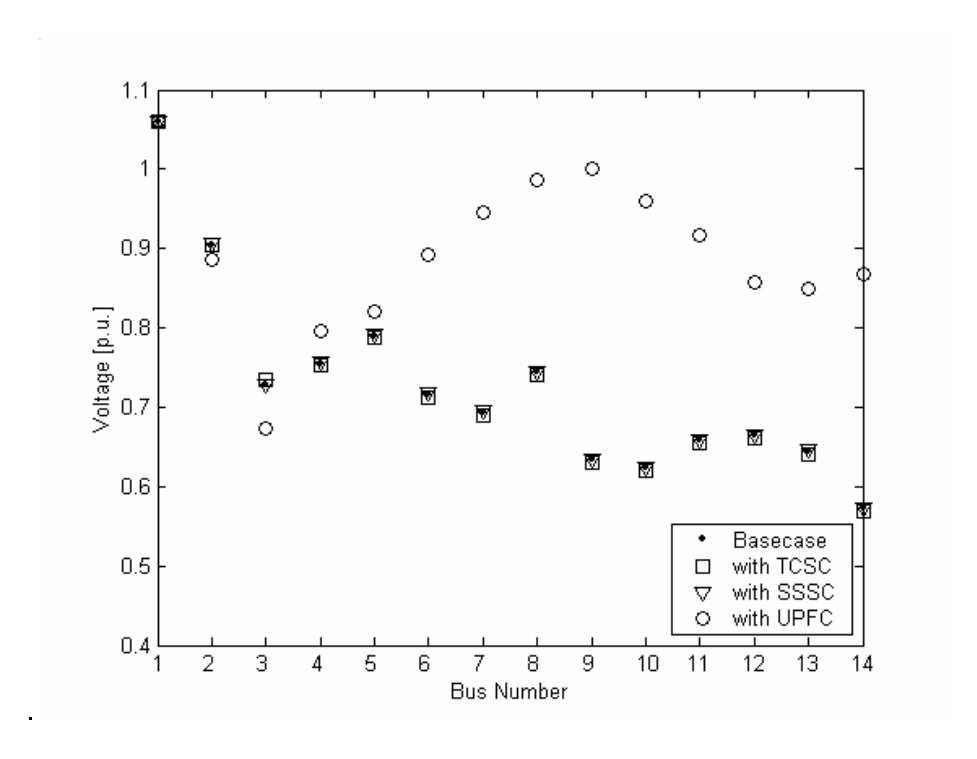


Figure 3.15: Voltage profile of base case, with TCSC, SSSC and UPFC.

#### 3.3.4 Power Losses

Real and reactive power losses of the system at various loading factors are shown in Figures 3.16 and 3.17, respectively. From Figures 3.16 and 3.17, the real and reactive power losses appear to be following the same pattern in this test system. At the higher loading factor, both real and reactive power losses increase very rapidly. The increase of losses near the collapse point is lowest in the case of UPFC and highest in the base case. Compared with TCSC and SSSC, UPFC gives lower loss increase at higher LM.

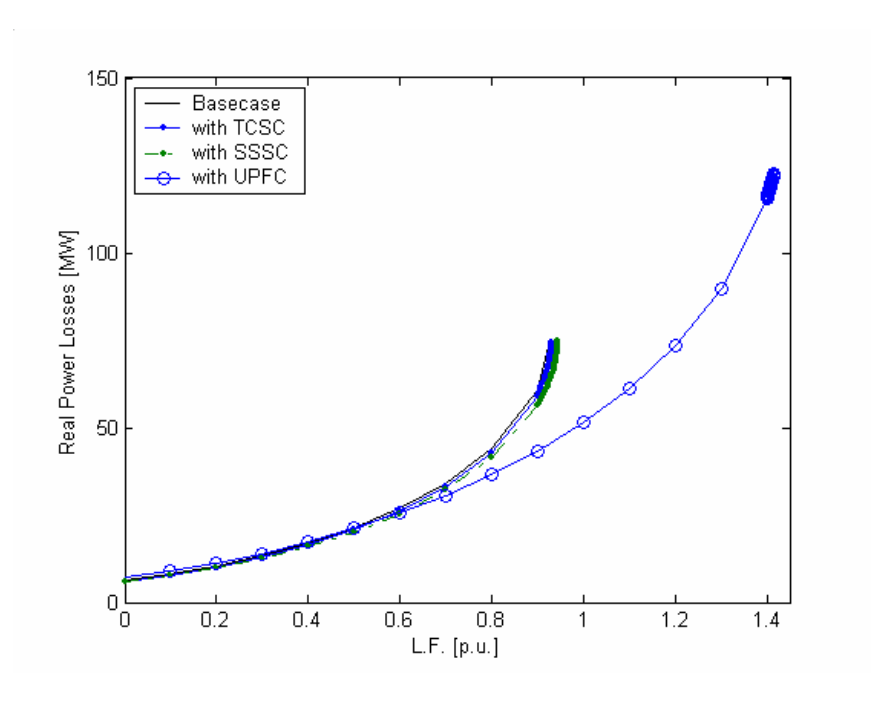


Figure 3.16: Real power losses of the system with STATCOM, SSSC and UPFC.

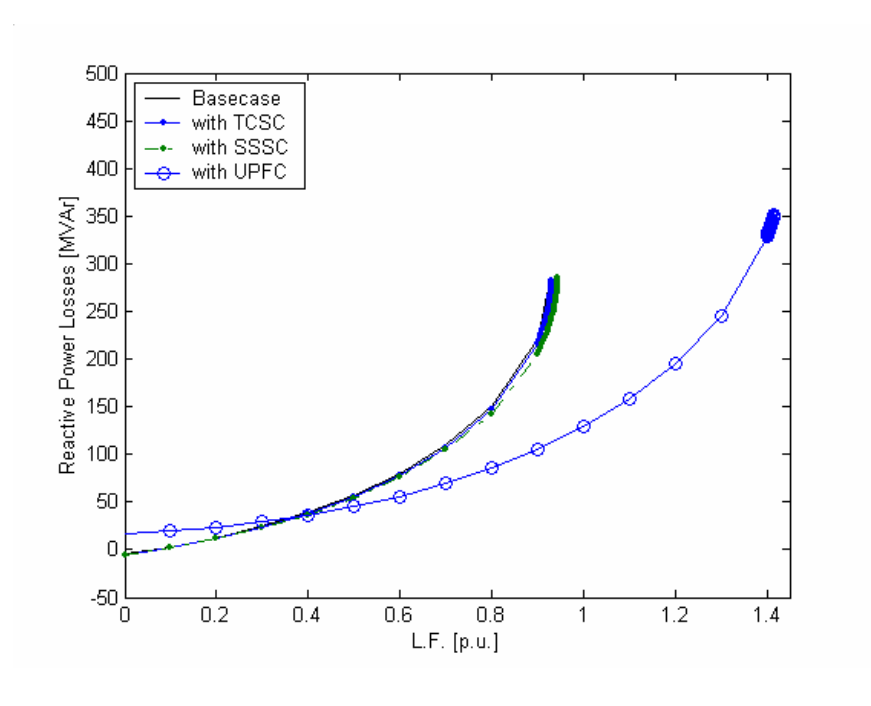


Figure 3.17: Reactive power losses of the system with TCSC, SSSC and UPFC.

#### 3.3.5 Contingency

Loading Margin of three worst contingencies are tabulated in Table 3.8 for base case, TCSC, SSSC and UPFC. LM of line 1-2 and 1-5 contingencies can not be obtained for the case of TCSC and SSSC since they are installed at line 1-5. There are only two path, through lines 1-2 and 1-5, that most of the generation can be transferred to the load. From Table 3.8, TCSC and SSSC can slightly increase LM for line 2-3 contingency. UPFC, on the other hand, provides much improvement in terms of LM for all the contingency cases.

Table 3.8: Loading Margin for various line outages for base case and different controllers

Case	Loading Margins [p.u.] for line outages			
	1-2	2-3	1-5	
Base Case	0.25184	0.38278	0.59605	
TCSC	-	0.4033	-	
SSSC	-	0.3964	-	
UPFC	0.5003	0.5596	1.0161	

#### 3.4 Comparison of FACTS Controllers

#### 3.4.1 PV Curves and Voltage Profiles

In this section, various FACTS controllers are compared. Figure 3.18 shows PV curves of base case and system with FACTS devices for the modified IEEE 14-bus test system. LM of base case and various FACTS devices are shown in Table 3.9. From Figure 3.18 and Table 3.9, UPFC gives the highest LM improvement followed by shunt FACTS devices and series FACTS devices, respectively. The IEEE 14-bus test system requires reactive power compensation at the distribution level, thus installing shunt reactive devices could provide higher LM than series devices. UPFC, on the other hand, is composed of both shunt and series devices. Introducing UPFC can provide reactive power both at the distribution level and at the line, thus making the device the most effective one in the terms of LM improvement in this test system.

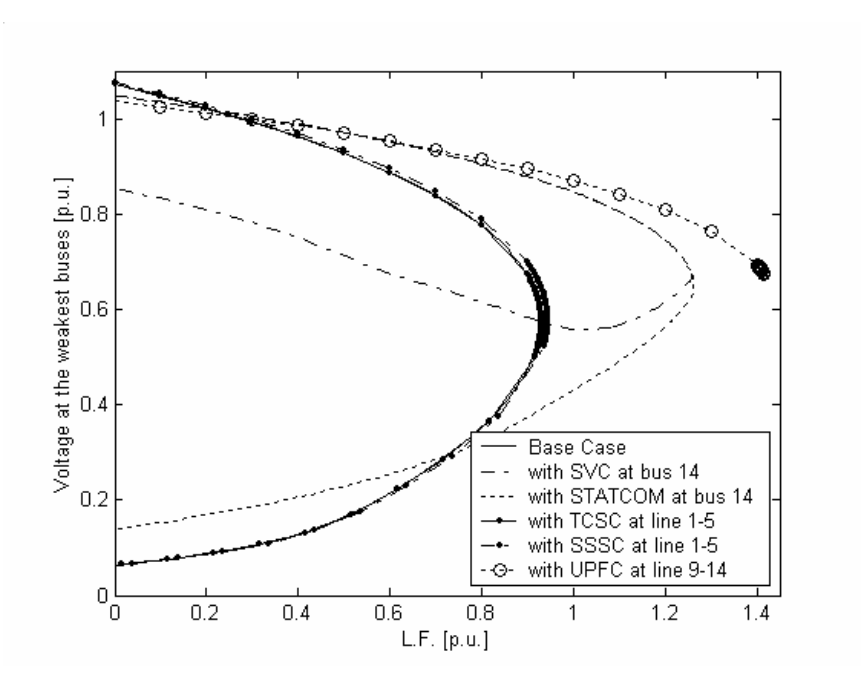


Figure 3.18: PV curves of base case, with FACTS devices.

Table 3.9: LM and % Increase of LM of base case, with FACTS devices

Case	Loading Margin [p.u]	% Increase of LM from base case
Base Case	0.9278	-
SVC	1.2606	35.9
STATCOM	1.2625	36.1
TCSC	0.9307	0.3
SSSC	0.9452	1.9
UPFC	1.4165	52.7

Voltage profiles at the LM of base case and various FACTS devices are illustrated in Figure 3.19. From Figure 3.19, it can be seen that UPFC provides better voltage profiles than other FACTS devices with higher LM. Compared to series FACTS devices, shunt devices give better voltage profiles since the reactive power is introduced at the weakest bus.

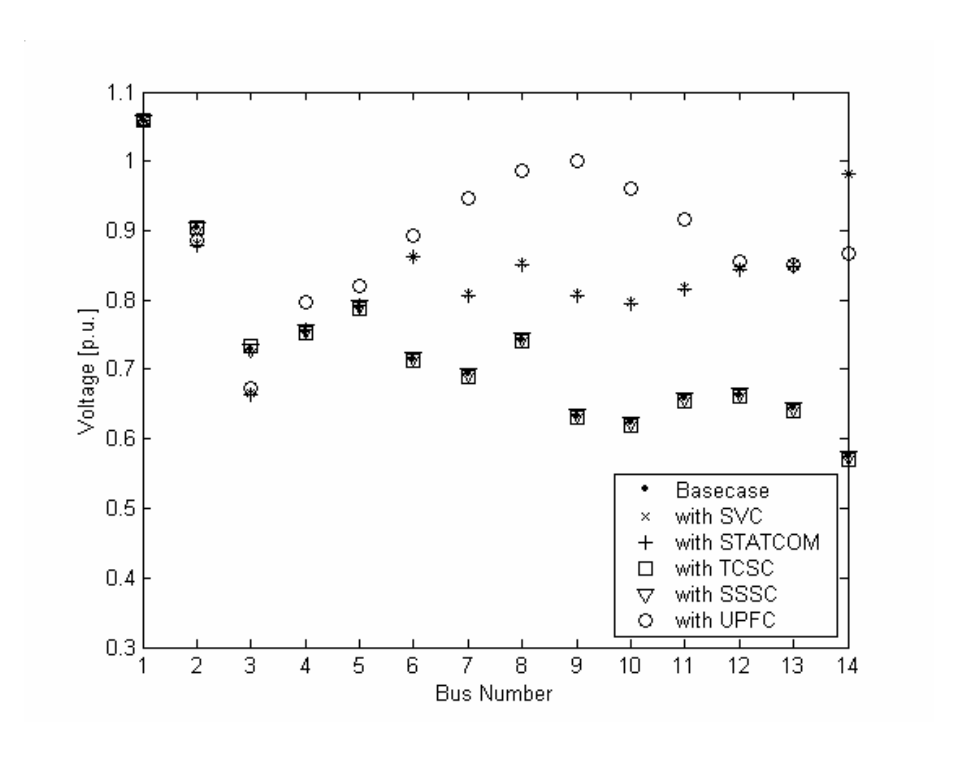


Figure 3.19: Voltage profile of base case, with FACTS devices.

#### 3.4.2 Power Losses

Real and reactive power losses occurred in the system are plotted in Figures 3.20 and 3.21, respectively. From Figures 3.20 and 3.21, both real and reactive power losses follow the same pattern at various LFs. UPFC has lower losses as well as the incremental losses compared to other FACTS devices, thus giving highest LM and better voltage profile. Shunt FACT devices provide lower losses compared to series FACTS devices and base case.

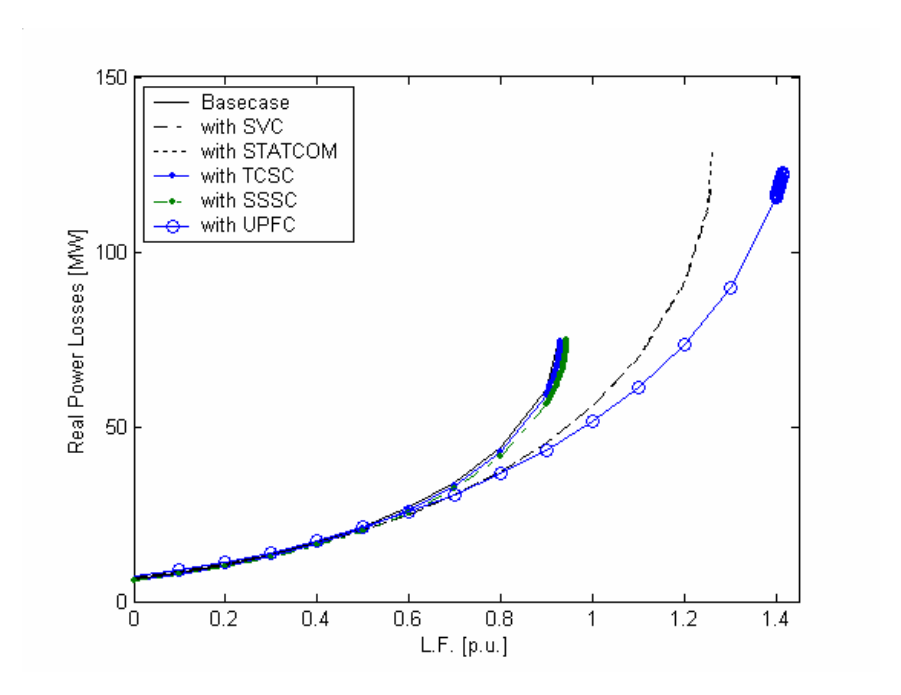


Figure 3.20: Real power losses of the system with FACTS devices.

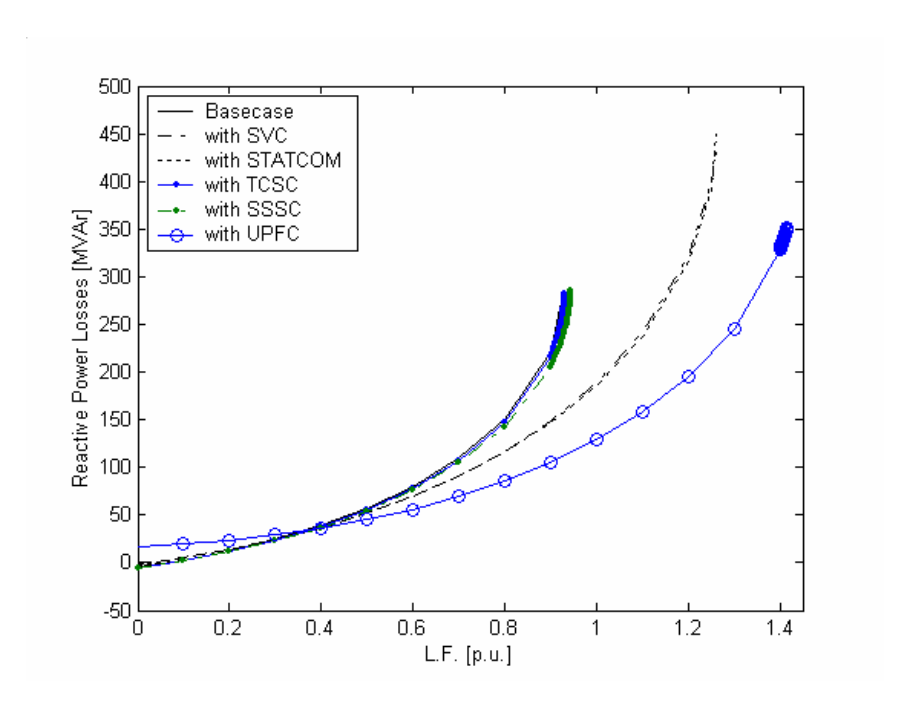


Figure 3.21: Reactive power losses of the system with FACTS devices.

#### 3.4.3 Contingency

LMs for three worst contingency cases are shown in Table 3.10 for various FACTS devices. From Table 3.10, shunt FACTS devices provide higher LM than series FACTS devices for all contingency cases, as the system requires reactive power at the load location. UPFC is the device that gives the highest voltage stability margin improvement.

Table 3.10: Loading Margin for various line outages for base case and various FACTS controllers

Case	Loading Margin	Loading Margins [p.u.] for line outages				
Cuse	1-2	2-3	1-5			
Base Case	0.25184	0.38278	0.59605			
SVC	0.40205	0.49212	0.87061			
STATCOM	0.40097	0.49174	0.86916			
TCSC	-	0.4033	-			
SSSC	-	0.3964	-			
UPFC	0.5003	0.5596	1.0161			

#### 3.5 Summary

In this chapter, influence of various FACTS controllers on static voltage stability margin is thoroughly investigated. Two important issues associated with FACTS applications for voltage stability improvement, namely placement and sizing, are discussed in details for each type of FACS devices. Shunt FACTS devices, SVC and STATCOM, are compared first. Series FACTS devices, TCSC and SSSC, along with UPFC are compared next. Finally, all the devices are compared for loading margin, voltage profile and losses. The influence of these devices on static voltage stability margin under the worst contingency condition is also included.

## Chapter 4

#### **Conclusions**

### 4.1 Concluding Observations

This research has presented the influence of FACTS controllers in static voltage stability margin enhancement. The new ideas proposed are applied to IEEE 14 bus test system to see the usefulness of the methods. Further to observations and discussions, the following conclusions are made:

- (i) The shunt FACTS devices can increase voltage stability margin of the system more than series FACTS devices, as the weakest bus is in the distribution level. Among all the FACTS devices, UPFC provides highest loading margin followed by STATCOM and SSSC.
- (ii) Placement techniques for various FACTS devices are presented to increase voltage stability margin. Methodologies for identifying the best locations for series FACTS devices and UPFC are proposed. The appropriate location for shunt FACTS devices is the weakest bus of the system as well known. Series FACTS devices should be placed at the weakest line where the sensitivity of reactive power losses is the highest. UPFC controller location can be found from groups of weakest buses and weakest lines, which are obtained from placement techniques of shunt and series FACTS devices.
- (iii) The appropriate sizes or capacities of FACTS devices are also studied. Capacities of shunt FACTS devices can be found from amount of reactive power generated at the maximum loading point from the synchronous compensator. Another method is to find the relationship between LM and the corresponding capacities that shunt FACTS devices can deliver without having the voltage collapse. Capacities of TCSC, SSSC and UPFC can be found from amount of active and reactive power required at the collapse point.

#### 4.2 Main Contributions

The major contributions of this research can be summarized as follows:

- (i) Voltage stability assessments of various FACTS devices are studied and compared in the same test system. AC and DC representation of FACTS devices are used throughout the study.
- (ii) Methodologies to determine capacities and locations of FACTS devices and UPFC are proposed.

#### **4.3** Future Directions

There are numbers of issues that are still to be addressed in FACTS controllers in static voltage stability study:

- (i) Coordination and interaction of various FACTS devices related to static voltage stability can be studied to provide composite enhanced performance of these devices. Moreover, mathematical representation of capacities and locations may be investigated for the use of a full optimization technique to find the most appropriate size and location.
- (ii) Due to the expensive nature of FACTS controllers, a thorough cost-benefit analysis can be carried out to justify the economic viability of these controllers by translating various benefits of the use of the controllers on system performance in terms of money. This would be a useful contribution in the framework of deregulated market environment.

#### **BIBLIOGRAPHY**

- 1. B. Gao, G.K. Morison, P. Kundur, "Towards The Development of a Systematic Approach for Voltage Stability Assessment of Large-Scale Power Systems", *IEEE Transactions on Power System*, Vol. 11, No. 3, pp. 1314-1324, August 1996.
- 2. 13. T. Nagao, K. Tanaka and K. Takenaka, "Development of static and simulation programs for voltage stability studies of bulk power system", *IEEE Transactions on Power System*, Vol. 12, No. 1, pp. 273-281, February 1997.
- 3. IEEE/PES Power System Stability Subcommittee, *Voltage Stability Assessment: Concepts, Practices and Tools*, special publication, August 2003.
- 4. P. Kundur, Power System Stability and Control, McGrawHil, 1994.
- 5. Blackout of 2003: Description and Responses, Available: http://www.pserc.wisc.edu/.
- 6. C. A. Canizares, A. C. Z. DeSouza, and V. H. Quintana, "Comparison of performance indices for detection of proximity to voltage collapse", *IEEE Transactions on Power System*, Vol. 11, No. 3, pp. 1441-1447, August 1996.
- 7. P-A. Lof, G. Andersson and D. J. Hill, "Voltage stability indices for stressed power systems", *IEEE Transactions on Power System*, Vol. 8, No. 1, pp. 326-331, February 1993.
- 8. K. N. Srivastava, S. C. Srivastava and P. K. Kalra, "Prediction of voltage collapse in an integrated AC-DC network using the singular-value decomposition concept", *Electric Power System Research*, Vol. 28, pp. 111-122, 1993.
- 9. B. H. Lee and K. Y. Lee, "A Study on Voltage Collapse Mechanism in Electric Power Systems," *IEEE Transactions Power System*, Vol. 6, pp. 966-974, August 1991.
- 10. C.A. Canizares, A. C. Z. De Souza, and V. H. Quintana, "Comparison of performance indices for detection of proximity to voltage collapse," *IEEE Transactions Power System*, Vol. 11, No. 3, pp. 1441-1447, August 1996.
- 11. A. Sode-Yome and N. Mithulananthan, "Comparison of shunt capacitor, SVC and STATCOM in static voltage stability margin enhancement," *International Journal of Electrical Engineering Education*, UMIST, Vol. 41, No. 3, July 2004.
- 12. B. H. Lee and K. Y. Lee, "Dynamic and Static Voltage Stability Enhancement of Power Systems," *IEEE Transactions on Power Systems*, Vol. 8, No. 1, pp. 231-238, 1993.
- 13. Sode-Yome and N. Mithulananthan, "Maximizing static voltage stability margin in power systems using a new generation pattern", *Australasian Journal of Electrical & Electronics Engineering*, Vol. 2, No 3, 2005.
- 14. Cigre 95 TP108, FACTS Overview, IEEE Power Engineering Society, 1995.

- 15. Canizares and Z. T. Faur, "Analysis of SVC and TCSC Controllers in Voltage Collapse", *IEEE Transactions on Power Systems*, Vol. 14, No. 1, pp. 158-165, February 1999.
- 16. C. A. Canizares, "Power flow and transient stability models of FACTS controllers for voltage and angle stability studies", *IEEE/PES WM on Modeling, Simulation and Applications of FACTS Controllers in Angle and Voltage Stability Studies*, Singapore, January 2000.
- 17. D. Thukaram and A. Lomi, "Selection of Static VAR Compensator Location and Size for System Voltage Stability Improvement", *Electrical Power Systems Research*, Vol. 54, pp. 139-150, 2000.
- 18. M. H. Haque, "Optimal location of shunt FACTS devices in long transmission lines", *IEE Proceeding-Generation, Transmission*, *Distribution*, Vol. 147, No. 4, pp. 218-222, July 2000.
- 19. S. Ibrahim and A. Abusorrah, "Optimal allocation of SVCs for improvement of power system performance", *Electric Power Components and Systems*, Vol. 31, pp. 27-46, 2003.
- 20. S. Chang and J. S. Huang, "Optimal SVC placement for voltage stability reinforcement", *Electric Power System Research*, Vol. 42, pp. 165-172, 1997.
- 21. S. N. Singh and A. K. David, "A new approach for placement of FACTS devices in open power markets", *IEEE Power Engineering Review*, September 2001.
- 22. N. Amjady and M. Esmaili, "Improving voltage security assessment and ranking vulnerable buses with consideration of power system limit", Electric Power System Research, Vol. 25, pp. 705-715, 2003.
- 23. N. Amjady and M. Esmaili, "Voltage security assessment and vulnerable bus ranking of power systems", *Electric Power System Research*, Vol. 64, pp. 227-237, 2003.
- 24. Leita da Silva, I. P. Coutinho, A. C. Z. De Souza, R. B. Prada and A. M. Rei , "Voltage collapse risk assessment", *Electric Power System Research*, Vol. 54, pp. 221-227, 2000.
- 25. K. Y. Lee, A. Sode-Yome, and J. H. Park, "Adaptive Hopfield neural networks for economic load dispatch", *IEEE Transaction on Power System Apparatus and Systems*, Vol. 13, No. 2, pp. 519-526, August 1995.
- 26. K. Y. Lee, F. M. Nuroglu, and A. Sode-Yome, "Real power optimization with load flow using adaptive Hopfield neural networks", *Journal of Engineering Intelligent Systems*, Vol. 8, No. 1, pp. 53-58, March 2000.
- 27. J. Wood and B. F. Wollenberg, *Power Generation Operation & Control*, John Wiley & Sons, 1984.

- 28. Z. Fend, V. Ajjarpu and D. J. Maratukulam, "A practical minimum load shedding strategy to mitigate voltage collapse", IEEE Transactions on Power Systems, Vol. 13, No. 4, pp. 1285-1291, November 1998.
- 29. Bompard, E. Carpaneto, G. Chicco and R. Napoli, "Evaluation of the critical load increase direction in voltage collapse studies", *Electric Power System Research*, Vol. 43, pp. 61-67, 1997.
- 30. G. M. Huang and N. K. C. Nair, "Voltage stability constrained load curtailment procedure to evaluate power system reliability measures", *Proceeding of IEEE Power Engineering Society-Winter Meeting*, New York, January 2002, pp. 761-765.
- 31. C. L. DeMarco and T. J. Overbye, "An energy based security measure for assessing vulnerability to voltage collapse", *IEEE Transactions on Power System*, Vol. 5, No. 2, pp. 419-425, May 1990.
- 32. C. A. Canizares, F. L. Alvarado, C. L. Demarco, I. Dobson and W. F. Long, "Point of collapse methods applied to AC/DC power systems", *IEEE Transactions on Power System*, Vol. 7, No. 2, pp. 673-683, May 1992.
- 33. C. A. Canizares and F. L. Alvarado, "Point of collapse and continuation methods for large AC/DC systems", *IEEE Transactions on Power System*, Vol. 8, No. 1, pp. 1-8, February 1993.
- 34. C. Z. De Souza, "Tangent vector applied to voltage collapse and loss sensitivity studies", *Electric Power System Research*, Vol. 47, pp. 65-70, 1998.
- 35. C. Z. De Souza, "Discussion on some voltage collapse indices", *Electric Power System Research*, Vol. 53, pp. 53-58, 2000.
- 36. M. H. Haque, "Determination of steady-state voltage stability limit using P-Q curve", *IEEE Power Engineering Review*, pp.71-72, April 2002.
- 37. M. H. Haque, "Novel method of accessing voltage stability of a power system using stability boundary in P-Q plane, *Electric Power System Research*, Vol. 64, pp. 35-40, 2003.
- 38. K. P. Basu, "Power transfer capability of transmission line limited by voltage stability: simple analytical expressions", *IEEE Power Engineering Review*, pp. 46-47, September 2000.
- 39. K. Vu, M. M. Begovic, D. Novosel and M. M. Saha, "Use of local measurement to estimate voltage-stability margin", *IEEE Transactions on Power System*, Vol. 14, No. 3, pp. 1029-1035, August 1999.
- 40. T. J Overbye, "Use of FACTS devices for power system stability enhancement," *Proceedings of the 36th Midwest Symposium on Circuits and Systems*, Vol.2, 1993, pp.1019 1022.

- 41. M. Z. El-Sadek, M. M. Dessouky, G. A. Mahmoud and W. I. Rashed, "Enhancement of steady-state voltage stability by static VAR compensator", *Electric Power System Research*, Vol. 43, pp. 179-185, 1997.
- 42. C. A. Canizares, E. Uzunovic and J. Reeve and B. K. Johnson, "Transient stability and power flow models of the unified power flow controller for various control strategies," Technical Report 2004-9, University of Waterloo, Waterloo, March 2004.
- 43. A. Del Rosso, C. A. Canizares, V. Quintana and V. Dona, "Stability improvement using TCSC in radial power systems," *Proceedings of the North American Power Symposium (NAPS)*, Waterloo, ON, October 2000, pp. 12-32 12-39.
- 44. M. Rahman, M. Ahmed, R. Gutman, R. J. O'Keefe, R. J. Nelson and J. Bian, "UPFC application on the AEP system: planning consideration", *IEEE Transactions on Power System*, Vol. 12, No. 4, pp. 1695-1701, November 1997.
- 45. E. Uzunovic, C. A. Canizares and J. Reeve, "Fundamental frequency model of unified power flow controller," *Proceedings of the North American Power Symposium (NAPS)*, Cleveland, Ohio, October 1998, pp. 294-299.
- 46. B. T. Ooi, M Kanzerani, R. Marceau, Z. Wolanski, F.D. Galiana, D. McGillis and G. Joos, "Mid-point siting of FACTS device in transmission lines", *IEEE Transactions on Power Delivery*, Vol. 12, No. 4, pp. 1717-1722, October 1997.
- 47. C. P. Gupta, S. C. Srivastava and R. K. Varma, "Enhancement of static voltage stability margin with reactive power dispatch using FACTS devices", *13<sup>th</sup> PSCC*, Trondheim, June 28-July 2, 1999.
- 48. N. K. Sharma, R. K. Varma, and A. Ghosh, "Placement strategy for FACTS devices," *11<sup>st</sup> National Power Systems Conference*, Bangalor, India, December 2000, pp. 57-62.
- 49. S. Green, I. Dobson and F. L. Alvarado, "Sensitivity of Loading Margin to Voltage Collapse with respect to Arbitrary Parameters," *IEEE Transactions Power Syst*, Vol. 12, No. 1, pp. 262-272, Feb. 1997.
- 50. L.C.P. da Silva, Y. Wang, V.F. da Costa and W. Xu, "Assessment of Generator Impact on System Power Transfer Capability Using Modal Participation Factors", *IEE Proceedings Generation, Transmission and Distribution*, Vol. 149, Issue 5, pp. 564-570, Sept. 2002.
- 51. R. Wang and R. H. Lasseter, "Re-dispatching generation to increase power system security margin and support low voltage bus," *IEEE Transactions Power System*, Vol. 15, No. 2, pp. 496-501, May 2000.
- 52. O. Ekwue, H. B. Wan, D. T. Y. Cheng and Y. H. Song, "Voltage stability analysis on the NGC system", *Electric Power System Research*, Vol. 47, pp. 173-180, 1998.
- 53. J. G. Calderon-Guizar, G. A. Inda-Ruiz, and G. E. Tovar, "Improving the steady-state loading margin to voltage collapse in the North-West control area of Mexican power system", *Electric Power System Research*, Vol. 25, pp. 643-649, 2003.

- 54. T. V. Cutsem and R. Mailhot, "Validation of a fast voltage stability analysis method on the Hydro-Quebec system", *IEEE Transactions on Power System*, Vol. 12, No. 1, pp. 282-292, February 1997.
- 55. M. Khiat, A. Chaker, A. G. Exposito, J. L. Martinez Ramo, "Reactive power optimization an voltage control in the western Algerian transmission system: a hybrid approach", *Electric Power System Research*, Vol. 64, pp. 3-10, 2003.
- 56. Z. Khan, "A discussion and analysis of the voltage stability problems in Oman", *Electric Power System Research*, Vol. 49, pp. 31-36, 1999.
- 57. Feng and W. Xu, "Fast computation of post-contingency system margins for voltage stability assessment of large-scale power systems", *IEE Proceeding-Generation, Transmission*, *Distribution*, Vol. 147, No. 3, pp. 76-80, March 2000.
- 58. Z. De Souza, J. C. S. De Souza and A. M. L. De Silva, "On-line voltage stability monitoring", *IEEE Transactions on Power Systems*, Vol. 15, No. 4, pp. 1300-1305, November 2000.
- 59. C. A. Cañizares, et al., *UWPFLOW: Continuation and Direct Methods to Locate Fold Bifurcations in AC/DC/FACTS Power Systems*, University of Waterloo, available at http://www.power.uwaterloo.ca, Sept. 2004.
- 60. Matlab Functions, available at http://www.mathworks.com, June 2004.
- 61. A. Sode-Yome, V. Pothiratana and N. Mithulananthan, "Roles of small power producers as part of peak serving scheme," invited paper, *Power-Gen Asia 2004*, Bangkok, Oct. 5-7, 2004.
- 62. W. D. Rosehart, C. A. Canizares, and V. H. Quintana, "Effect of detailed power system models in traditional and voltage-stability-constrained optimal power-flow problems," *IEEE Transactions Power System*, Vol. 18, No. 1, pp. 27-35, February 2003.
- 63. F. Cazals and M. Pouget, "Estimating differential quantities using polynomial fitting of osculating jets", *Proceedings of the Eurographics/ACM SIGGRAPH symposium on Geometry processing*, Aachen, Germany, 2003, pp. 177-187.

## Appredix A

## **IEEE 14-Bus Test System**

```
14 BUS TEST SYSTEM:
C
C
               WSCC data file
C
C Case Title (3 A8 lines)
HDG
 14 BUS AC TEST SYSTEM
 WSCC/ETMSP DATA FORMAT
 NOVEMBER 2002
BAS
C
C
C System Data
C
C
                    AC BUSES
C
C Bus Input Data:
C - Type (A2) -> "B " -> PQ load bus
C
          "BQ" -> PV generator bus with Q limits
C
          "BE" -> PV generator bus with no Q limits
C
          "BV" -> PQ generator bus with V limits
C
          "BG" -> PQ generator bus with Q limits controlling voltage on
C
               a remote PV load bus
C
          "BC" -> PV load bus with remote voltage control
C
          "BT" -> PQ load bus with voltage controlled by LTC transformer
C
          "BS" -> Swing bus
C - Ow (A3) -> Owner
C - Name (A8) -> Bus Name
C - kV (F4.0) -> Bus kV base
C - Z(2A) \rightarrow Zone
C - PL (F5.0) -> P load in MW
C - QL (F5.0) -> Q load in MVars
C - SHUNT (2F4.0) -> MW and MVars shunts (+ for Capacitors)
C - PM (F4.0) -> Max. generator P power in MW
C - P (F5.0) -> generator P power in MW
C - QM (F5.0) -> Max. generator Q power in MVars (not needed for "BE"
C - Qm (F5.0) -> Min. generator Q power in MVars (not needed for "BE"
          PV bus types)
C - Vpu (F4.3)-> PV desired voltage magnitude in p.u. (max. voltage for
           "BV" PV bus type)
C - Vm (F4.3) -> Min. voltage for "BV" PV bus type.
C - Remote Name (A8) -> Remote controlled bus name for "BG" type bus.
C - Remote kV (F4.0) -> Remote controlled bus kV for "BG" type bus.
C - Remote %Q (I3) \, -> Percentage of Q of remote bus control for "BG" type bus.
                  3
                               5
                                           7
```

```
C
                 | SHUNT |
                                         REMOTE BUS
C \hspace{0.1cm} |Ow| Name \hspace{0.1cm} |kV\hspace{0.1cm}| Z|PL\hspace{0.1cm} |QL\hspace{0.1cm}| MW\hspace{0.1cm} |Mva|PM\hspace{0.1cm} |P\hspace{0.1cm}| QM\hspace{0.1cm} |Qm\hspace{0.1cm}| Vpu|Vm\hspace{0.1cm} |Name\hspace{0.1cm}| kV\hspace{0.1cm} |\%\hspace{0.1cm} Q
     BUS_1 69.0IE.0000.0000.000.0009999232.6990.0 -9891060 0
                                                                      0.0
     BUS_2 69.0IE21.7012.70.000.000999940.0050.00-40.01045 0
                                                                      0.0
BO
BO
     BUS_3 69.0IE94.2019.00.000.0009999.000040.00.00001010 0
                                                                      0.0
В
     BUS_4 69.0IE47.804.000.000.000.000.0000.0000.0000 0 0
                                                                      0.0
В
     BUS_5 69.0IE7.6001.600.000.000.000.0000.0000.0000 0 0
                                                                      0.0
    BUS_6 13.8IE11.207.500.000.0009999.000024.00-6.001070 0
BO
                                                                      0.0
В
     0.0
BQ
    BUS_8 18.0IE.0000.0000.000.0009999.000024.00-6.001090 0
                                                                      0.0
     BUS_9 13.8IE29.5016.60.000.000.000.0000.0000.0000 0 0
В
                                                                      0.0
     BUS_10 13.8IE9.0005.800.000.000.000.0000.0000.0000 0 0
                                                                      0.0
В
     BUS_11 13.8IE3.5001.800.000.000.000.0000.0000.0000 0 0
В
                                                                      0.0
В
     BUS_12 13.8IE6.1001.600.000.000.000.0000.0000.0000 0 0
                                                                      0.0
     BUS_13 13.8IE13.505.800.000.000.000.0000.0000.0000 0 0
В
                                                                      0.0
     BUS_14 13.8IE14.905.000.000.000.000.0000.0000.0000 0 0
В
                                                                      0.0
C
C
C
                    AC LINES
C
C Line Input Data:
C - Type (A2) -> "L "
C - Ow (A3) -> Owner
C - Name_1 (A8) -> Name of sending bus
C - kV1 (F4.0) -> kV base for sending bus
C - M (I1) -> Metered bus for flow interchange
C - Name_2 (A8) -> Name of receiving bus
C - kV2 (F4.0) -> kV base for receiving bus
C - C (I1) -> Circuit ID
C - S (I1) -> Section number
C - In (F4.0) -> Rated Amps.
C - N (I1) -> Circuit number
C - R (F6.5) -> p.u. series R of PI equivalent
C - X (F6.5) -> p.u. series X of PI equivalent
C - G/2 (F6.5) -> p.u. shunt G/2 of PI equivalent
C - B/2 (F6.5) -> p.u. shunt B/2 of PI equivalent
C - Mil (F4.1) -> Length in miles
C
C
                              5
                                          7
                  3
                                    6
\mathbf{C}
                   CS N
C \hspace{0.2cm} |Ow|Name\_1\hspace{0.2cm}|kV1||Name\_2\hspace{0.2cm}|kV2|||In\hspace{0.2cm}||\hspace{0.2cm}R\hspace{0.2cm}|\hspace{0.2cm}|X\hspace{0.2cm}|\hspace{0.2cm}|G/2\hspace{0.2cm}|\hspace{0.2cm}|B/2\hspace{0.2cm}|Mil|
   BUS_1 69.01BUS_2 69.011.0001.01938.05917.00000.02640
   BUS_1 69.01BUS_5 69.011.0001.05403.22304.00000.02460
   BUS 2 69.01BUS 3 69.011.0001.04699.19797.00000.02190
L
   BUS_2 69.01BUS_4 69.011.0001.05811.17632.00000.01870
L
   BUS_2 69.01BUS_5 69.011.0001.05695.17388.00000.01700
   BUS_3 69.01BUS_4 69.011.0001.06701.17103.00000.01730
L
   BUS_4 69.01BUS_5 69.011.0001.01335.04211.00000.00640
L
    BUS_6 13.81BUS_11 13.811.0001.09498.19890.00000.00000
```

```
BUS_6 13.81BUS_12 13.811.0001.12291.25581.00000.00000
   BUS_6 13.81BUS_13 13.811.0001.06615.13027.00000.00000
L
   BUS_7 13.81BUS_8 18.011.0001.00000.17615.00000.00000
   BUS_7 13.81BUS_9 13.811.0001.00000.11001.00000.00000
L
   BUS_9 13.81BUS_10 13.811.0001.03181.08450.00000.00000
L
   BUS_9 13.81BUS_14 13.811.0001.12711.27038.00000.00000
  BUS_10 13.81BUS_11 13.811.0001.08205.19207.00000.00000
   BUS_12 13.81BUS_13 13.811.0001.22092.19988.00000.00000
L
   BUS_13 13.81BUS_14 13.811.0001.17093.34802.00000.00000
L
\mathbf{C}
C
C
                 TRANSFORMERS
C
C Transformer Input Data:
C - Type (A2) -> "T "
C - Ow (A3) -> Owner
C - Name_1 (A8) -> Name of sending bus
C - kV1 (F4.0) -> kV base for sending bus
C - M (I1) -> Metered bus for flow interchange
C - Name_2 (A8) -> Name of receiving bus
C - kV2 (F4.0) -> kV base for receiving bus
C - C (I1) -> Circuit ID
C - S (I1) -> Section number
C - Sn (F4.0) -> Rated MVA
C - N (I1) -> Circuit number
C - R (F6.5) -> p.u. series R of equivalent circuit
C - X (F6.5) -> p.u. series X of equivalent circuit
C - G (F6.5) -> p.u. shunt G of equivalent circuit
C - B (F6.5) -> p.u. shunt B of equivalent circuit
C - Tap1 (F5.2) -> kV tap for sending bus
C - Tap2 (F5.2) -> kV tap for receiving bus
C
                      4
                            5
                3
                                        7
C
                  CS
C \hspace{0.2cm} |Ow|Name\_1 \hspace{0.2cm} |kV1||Name\_2 \hspace{0.2cm} |kV2|||Sn \hspace{0.2cm} |\hspace{0.2cm} R \hspace{0.2cm} |\hspace{0.2cm} X \hspace{0.2cm} |\hspace{0.2cm} G \hspace{0.2cm} |\hspace{0.2cm} B \hspace{0.2cm} |Tap1|Tap2|
   BUS 4 69.01BUS 7 13.811.0001.00000.20912.00000.0000067.4813.80
    BUS_4 69.01BUS_9 13.811.0001.00000.55618.00000.0000066.8613.80
   BUS_5 69.01BUS_6 13.811.0001.00000.25202.00000.0000064.3113.80
A IEEE14 BUS_2 69.0 0.00 IE
ZZ
\mathbf{C}
C
C
                SOLUTION CONTROL CARD
C
C Solution control card:
C - Max Iter (I5) -> Maximum number of Newton-Raphson iteration
C - Name (A8) -> Name of the slack bus
C - kV (F4.0) -> kV base for slack bus
C - Angle (F10.4) -> Reference angle for slack bus in degrees
```

```
C
C
C
1
2
3
4
5
6
7
8
C
345678901234567890123456789012345678901234567890123456789012345678901234567890123456789012345678901234567890123456789012345678901234567890123456789012345678901234567890123456789012345678901234567890123456789012345678901234567890123456789012345678901234567890123456789012345678901234567890123456789012345678901234567890123456789012345678901234567890123456789012345678901234567890123456789012345678901234567890123456789012345678901234567890123456789012345678901234567890123456789012345678901234567890123456789012345678901234567890123456789012345678901234567890123456789012345678901234567890123456789012345678901234567890123456789012345678901234567890123456789012345678901234567890123456789012345678901234567890123456789012345678901234567890123456789012345678901234567890123456789012345678901234567890123456789012345678901234567890123456789012345678901234567890123456789012345678901234567890123456789012345678901234567890123456789012345678901234567890123456789012345678901234567890123456789012345678901234567890123456789012345678901234567890123456789012345678901234567890123456789012345678901234567890123456789012345678901234567890123456789012345678901234567890123456789012345678901234567890123456789012345678901234567890123456789012345678901234567890123456789012345678901234567890123456789012345678901234567890123456789012345678901234567890123456789012345678901234567890123456789012345678901234567890123456789012345678901234567890123456789012345678901234567890123456789012345678901234567890123456789012345678901234567890123456789012345678901234567890123456789012345678901234567890123456789012345678901234567890123456789012345678901234567890123456789012345678901234567890123456789012345678901234567890123456789012345678901234567890123456789012345678901234567890123456789012345678901234567890123456789012345678901234567890123456789012345678901234567890123456789012345678901234567890123456789012345678901234567890123456789012345678901234567890123456789012345678901234567890123456789012345678901234567890123456789012345678901234
```

# Appendix B

## **FACTS Controller Data**

## C.1 SVC Data

$X_c$ (p.u.)	$X_l$ (p.u.)	$\alpha_{min}$ (deg.)	$\alpha_{max}(\deg.)$	Slope (%)	S (MVA)	kV
1.1708	0.4925	90	175	2	150	26

## C.2 STATCOM Data

$R_c$ (p.u.)	<i>R</i> (p.u.)	<i>X</i> (p.u.)	S (MVA)	k	$X_{sl}$ (%)
0.0017	0	0.145	150	0.9	2

## C.3 TCSC Data

$X_c(p.u.)$	$X_l$ (p.u.)	$\alpha_{min}$ (deg.)	$\alpha_{max}(\deg.)$	S (MVA)
10% of $X_l$	50% of the line	144	175	100

## C.4 SSSC Data

$R_c$ (p.u.)	<i>R</i> (p.u.)	<i>X</i> (p.u.)	S (MVA)	k
0.0017	0	0.145	100	0.9

## C.5 UPFC Data

## Shunt Part

$R_c$ (p.u.)	<i>R</i> (p.u.)	<i>X</i> (p.u.)	S (MVA)	k	$X_{sl}$ (%)
0.0017	0	0.145	150	0.9	2

## Series Part

$R_c$ (p.u.)	<i>R</i> (p.u.)	<i>X</i> (p.u.)	S (MVA)	k
0.0017	0	0.145	100	0.9